



Fermilab

FERMILAB TM-970

0102.000

The Injection System For
The Beijing Booster
Synchrotron

May 1980

Jiang Yan-ling, Shi Yin-Sheng, Xiao Yi-xuan, Zhang Chuang,
and Carlos Hojvat

Abstract

This Technical Memorandum includes the conceptual design and the details of most of the hardware components required for the injection system into the Beijing Booster Synchrotron of the Institute of High Energy Physics of the People's Republic of China.

The write-up is subdivided in six chapters: Theoretical Design, Calculations on the Stripping Foil, Magnet Design (Fast Orbumps and DC Septum), H^- Orbump Power Supply, Diagnostics and Summary. The design itself follows closely that of the Charge Exchange Injection for the Fermilab Booster accelerator. Throught the design emphasis has been put on utilizing components available in the People's Republic of China. It is hoped that many other components could be obtained from Chinese industry.

The most delicate part of the injection system is the stripping foil. Enough effort, not reported here, was put into the manufacturing techniques to enable the Beijing Institute to develop their own facilities. The mounting of foils to the specifications of this report was succesfully achieved by the chinese colleagues using foils manufactured in the U.S.A.

Some of the general mechanical design, to incorporate the injection system into the accelerator, is not covered by this note.

The Injection System for the
Beijing Booster Synchrotron

May 1980

Yan-ling Jiang, Yiu-sheng Shi, Yi-xuan Xiao, Chuang Zhang,
and Carlos Hojvat

Introduction

The present technical memorandum includes the conceptual design and the details of all the components required for the injection system into the Beijing Booster Synchrotron of the Institute of High Energy Physics of the People's Republic of China. This design incorporates "Charge Exchange Injection" and is similar in concept to the system operating now at Fermilab.

This TM is the result of more than 6 months of work by Yin-Sheng Shi, Yan-ling Jiang, Yi-Xuan Xiao, and Chuang Zhang of the Institute of High Energy Physics (Beijing) and Carlos Hojvat of Fermilab. Significant contributions to this report have been made by many persons at Fermilab, we hope that their contributions have all been duly acknowledged in the appropriate places. This note is subdivided as shown in the following outline.

OUTLINE

- I. THEORETICAL DESIGN
- II. CALCULATIONS ON THE STRIPPING FOIL
FOR THE BPS INJECTION SYSTEM
- III(a) MAGNET DESIGN - ORBUMPS
- III(b) MAGNET DESIGN - INJECTION SEPTUM
- IV. DESIGN OF THE H^- ORBUMP POWER SUPPLY
- V. DIAGNOSTICS
- VI. SUMMARY

CHAPTER 1

THEORETICAL DESIGN OF THE INJECTION SYSTEM FOR THE BEIJING BOOSTER SYNCHROTRON

C. Zhang

The Beijing Booster synchrotron is a rapid cycling synchrotron with a repetition rate of 12.5 Hz, an injection energy of 93 MeV, and an extraction energy of 2.0 GeV. The main parameters of the booster are summarized in Table I-1⁽¹⁾ together with the ones for the Fermilab booster⁽²⁾.

Figure I-1 shows the machine functions ($\alpha_p, \beta_H, \beta_v$) of the Beijing Booster.

From Table I-1 we can see that the ratio of the injection momenta of these two machines, $\frac{428}{644} = 0.66$, is approximately equal to the ratio of the long straight lengths of $\frac{4.1}{6.0} = 0.68$. So a similar injection system to the Fermi Booster can be adopted for the Beijing Booster.

The H^- charge exchange injection has been used successfully in ANL and FNAL⁽³⁾. It is based on the capture of protons by stripping electrons from H^- ions, or H^- atoms, on the closed orbit of the circular accelerator. The advantage of H^- injection is that it frees us from the limitations imposed by Liouville's theorem. Due to the opposite curvature of the injected H^- ions and circulating H^+ beam in a magnetic field, H^- ions can be injected during successive

turns into the same transverse phase space. H^- charge exchange injection can increase the phase density of the circulating beam with respect to the injected beam, to increase the intensity of the accelerator with acceptable beam loading of the linac. H^- charge exchange injection in the horizontal plane will be used in the Beijing Booster.

The injection takes place in the first cell of the booster. Several schemes ⁽¹⁾ ⁽⁴⁾ have been studied, and finally we have chosen the one utilizing a local horizontal orbit bump. In this scheme all the injection elements are located in the same long straight section as shown in Figure I-2. The local closed orbit distortion is limited within the range of one long straight section. The four equal "bumps" magnets can be excited in a series or parallel by the same power supply. This design requires a single type of magnet, and also simplifies the tracking problem between different magnets which is required in other schemes.

The 93 MeV H^- beam from the linac is bent in the injection septum MSI, emerging parallel to the closed orbit. The first two pulsed orbit bump magnets MBHI-1 and MBHI-2 are used to superimpose the trajectories of any circulating beam and the injected H^- beam. The mixed beam of protons and H^- ions traverses a stripping foil installed beyond the envelope of the circulating beam so as not to become an obstacle of normal acceleration. The two electrons are removed from most of the H^- ions and a beam mainly composed of protons emerges from the downstream side of the foil.

The stripped electrons are collected on an electrode. The proton beam is restored to the central orbit by pulsed orbumps MBHI-3 and MBHI-4 before entering the downstream F lattice magnet. These magnets separate the protons from other charge fractions of the beam during injection. H^- ions will be bent opposite to the circulating beam in case of foil breakage. Beam stops are used to collect the neutral and negative ions. One upstream of MBHI-4 collects the negative ions. Another one located downstream after the F magnet is used for the neutral beam. Here the horizontal envelope of the beam is less than 4 cm, and we can put a stop to collect H^0 without interfering with the circulating beam.

As the circulating beam must also traverse the stripping foil during and for some time after injections, multiple scattering in the foil results in emittance blow-up of the circulating beam. The fall time of the pulsed orbumps power supply must be as short as possible. These problems are discussed in the section covering the stripping foils.

The injected beam and injection point parameters are given in Table I-2, and in Table I-3 the parameters of the injection components are listed.

Due to the large deflection angle of the local closed orbit with respect to the central orbit, the edge effect of the orbumps will disturb the betatron oscillation, and the spread of stopbands will be increased. Estimation shows the half spread of stopbands due to the "orbumps" for a tune of $Q_v = 5$ to be only of $|P|_v \sim 0.03$.

In order to reach the designed intensity in the booster, it may be necessary to fill the transverse acceptances of the machine as uniformly as possible. In the vertical plane, scattering by the stripping foil and space charge effects accomplishes this, but other techniques may be required to fill the larger horizontal acceptance. As this will increase the complexity of the injection power supplies, in the beginning we will not use this scanning technique.

Assuming the H^- beam intensity from the linac to be 30 mA, an injection time of 30 μ s, and a booster transmission of about 50%, then the booster should be capable of delivering an intensity of about 2.8×10^{12} ppp.

References:

- 1) "The Preliminary Design of Beijing Proton Synchrotron (BPS)", BPS Staff, September 1979.
- 2) Booster Staff, E.L. Hubbard, Editor, "FNAL Booster Synchrotron", FNAL TM-405, January 1973.
- 3) "Discussion About the Injection System of Beijing Booster Synchrotron", Beijing Booster Staff Notes, December 1979.
- 4) C. Hojvat et al., "The Multiturn Charge Exchange Injection System for the Fermilab Booster Accelerator", IEEE, Vol. NS-26, No. 3, p. 3149, June 1979.

TABLE I-1. Machine Parameters of the Beijing
Booster Synchrotron and the Fermilab
Booster

Parameters	Unit	Beijing	Fermilab
Max. Energy	GeV	2.0	8.0
Inj. Energy (Momentum)	MeV (MeV/c)	93(428)	200(644)
Design Beam Intensity	ppp	2×10^{12}	4×10^{12}
Max. Bending Field	Gs	9412	6700
Lattice Type		FODOO-CF	FOFDOOD-CF
Mean Radius	m	22.3	75.5
Length of Long Straight Section	m	4.1	6.0
Betatron Osc. Freq. (QH/QV)		4.73/4.80	6.7/6.8
Transverse Acceptance	(H)	92π	25π
	(V) mm-mrad	40π	16π
$\frac{\Delta p}{p}$		2×10^{-3}	1.5×10^{-3}
β_H max	m	14.74	33.66
β_V max	m	14.52	20.46
β_H min	m	2.12	6.12
β_V min	m	2.06	5.27
η max	m	1.80	3.20
Beam Cross Section in	F	10.0*3.4	
	D cm*cm	6.0*5.6	

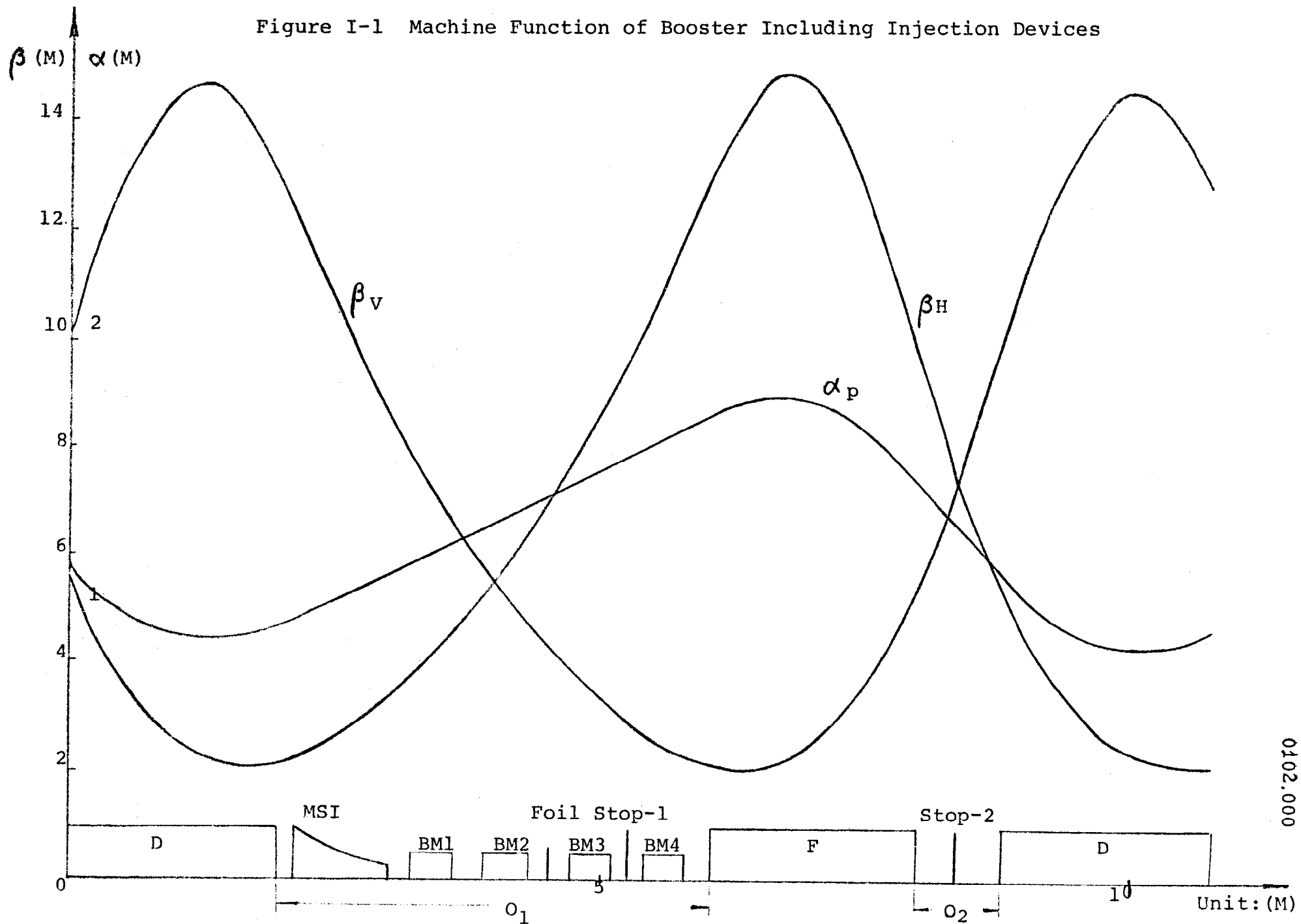
TABLE I-2. Injected Beam Quality and Injection Point Parameters

Injected Beam	Energy		MeV	93
	Current		mA	≥ 30
	Momentum Spread			$\pm 2 * 10^{-3}$
	Normalized Emittance	Horizontal Vertical	mm-mrad	8π 8π
Injection Time			μs	≥ 30
Injection Turns				≥ 26
Injection Point Parameters	Distance to Central Orbit		mm	55
	Slope of Closed Orbit		mrad	0
	α_x		rad	-1.583
	β_x		m	6.942
	α_z		rad	1.077
	β_z		m m	4.229
	η		m m	1.431
	η'		rad	0.1983

TABLE I-3. The Parameters of Injection Compoents

Parameters	Unit	Orbump	Septum
Deflection Angle	mrad	78.6	433.3
Field	Gs	2804	6874
Number		4	1
Length (each)	m	0.4	0.9
Aperture (H * V)	mm * mm	170 * 56	40 * 35
Fall Time	s	30	100 or D.C

Figure I-1 Machine Function of Booster Including Injection Devices



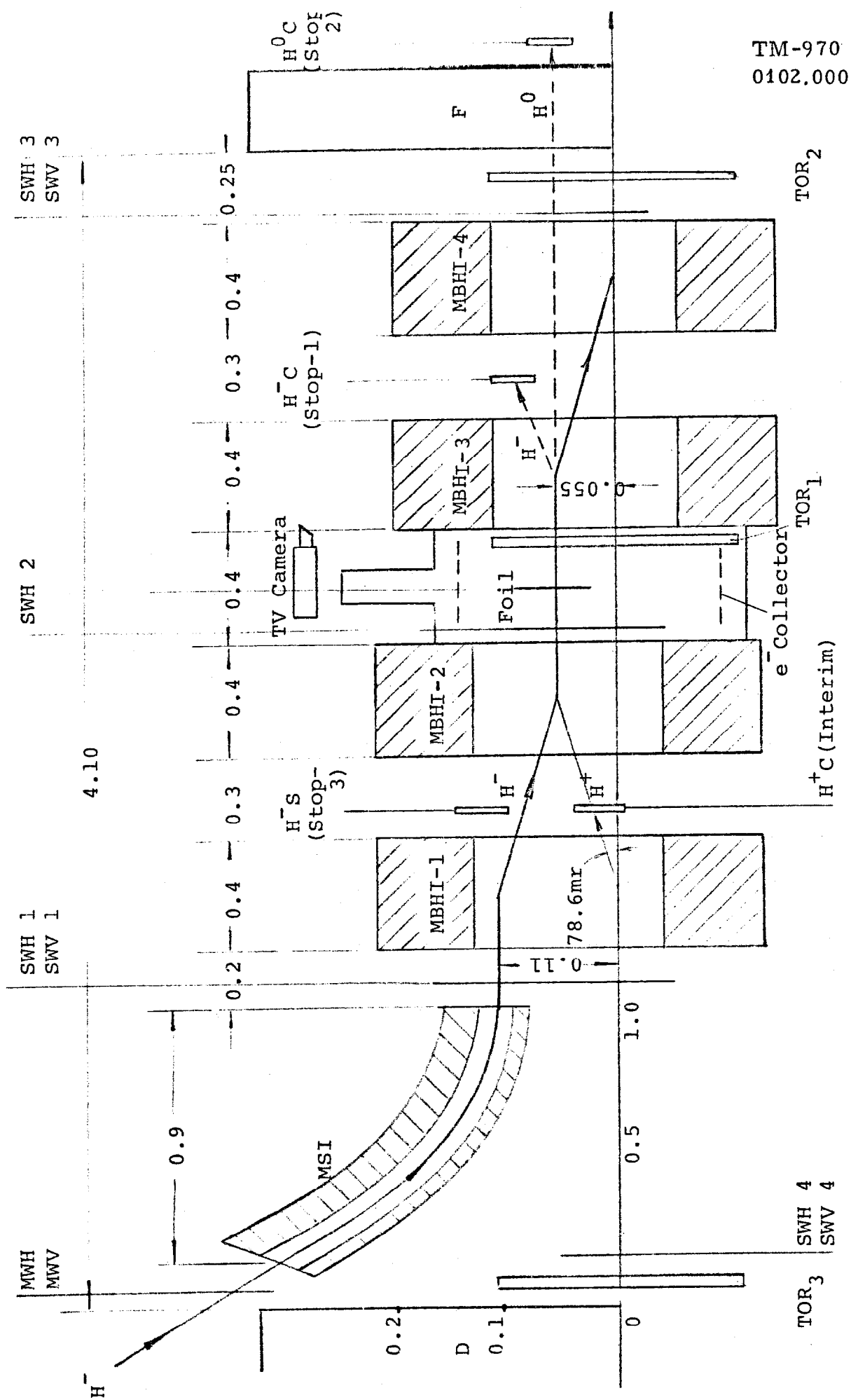


Figure I-2 Layout of the Booster Injection System (Distances are in meters)

CHAPTER II

CALCULATION ON THE STRIPPING FOIL FOR THE BPS INJECTION SYSTEM

Xiao Yi-xuan

II-1. H^- to H^+ Conversion Efficiency

When H^- ions traverse a material, six charge exchange processes can occur. Three are the electron loss reactions $(-1,0)$, $(0,1)$, $(-1,1)$, and three are the electron pickup reactions $(1,0)$, $(0,-1)$, $(1,-1)$. For energies above 100 keV the cross section for electron-pickup are very small and can be neglected⁽¹⁾. After H^- ions traverse a stripping foil there are three charge fractions N^- , N^0 , N^+ , in the beam. Three equations describe the variation of the charge fractions with the foil thickness.

$$N^- = e^{- (\sigma_{-10} + \sigma_{-11})n}$$

$$N^0 = \frac{\sigma_{-10}}{\sigma_{-10} + \sigma_{-11} - \sigma_{01}} e^{-\sigma_{01}n} - e^{- (\sigma_{-10} + \sigma_{-11})n}$$

$$N = 1 - N^- - N^0 \quad (II-1)$$

Where n is the number of target atoms per cm^2 and σ_{-10} , σ_{01} , σ_{-11} are the electron loss cross sections. Electron loss cross sections increase with atomic number and stripping efficiency N^+ increases with foil thickness.

For multiturn charge exchange injection into the Beijing Booster, the circulating beam must traverse the foil for at least as many times as the number of turns injected. Multiple scattering in the foil results in emittance blow-up of the circulating beam. The lower the atomic number, the lower the multiple scattering for a given stripping efficiency. Among others Lithium, Beryllium, Carbon and Aluminum foils are available. Both Lithium and Beryllium foils

are expensive and present handling problems. The choice is left between Carbon and Aluminum. Carbon not only gives rise to lower multiple scattering but is also cheaper than Aluminum⁽²⁾.

From C. Hojvat's measurement⁽³⁾ we can find the electron loss cross section of Carbon for H^- as a function of energy. For 93 MeV H^- we get:

$$\sigma_{-10} + \sigma_{-11} = 4 \times 10^{-18} \text{ cm}^2/\text{atom}$$

$$\sigma_{01} = 1.5 \times 10^{-18} \text{ cm}^2/\text{atom}$$

We can now calculate the values of N^- , N^0 , N^+ as a function of the thickness of the Carbon foils. The results are shown in Table II-1.

The stripping efficiency reaches 92% for a foil thickness of $40 \mu\text{g}/\text{cm}^2$. And it approaches 100% for a thickness of $100 \mu\text{g}/\text{cm}^2$.

Figure II-1 shows the charge fractions N^- , N^0 , N^+ , vs. foil thickness.

II-2. RMS Multiple Scattering Angle Versus Foil Thickness

The associated RMS multiple scattering angle is⁽⁴⁾

$$\langle \theta^2 \rangle^{1/2} = \frac{0.015}{\beta p} \left(\frac{x}{L_{\text{Rad}}} \right)^{1/2} \quad (\text{II-2})$$

$$\beta = \frac{v}{c} = \left(\frac{\gamma^2 - 1}{\gamma^2} \right)^{1/2} \text{ for 93 MeV protons} = 0.415$$

$$p = m (\gamma^2 - 1)^{1/2}$$

$$\text{for 93 MeV protons } p = 428 \times 10^{-3} \text{ GeV}/c$$

$$x = \text{foil thickness (gm/cm}^2\text{)}$$

$$L_{\text{Rad}} = \text{Radiation length of substance (gm/cm}^2\text{)}$$

$$\text{for Carbon: } L_{\text{Rad}} = 44.6 \text{ gm/cm}^2$$

A combination of equation (II-1) and (II-2) yields Table II-2 of the conversion efficiency and θ_{RMS} for Carbon foils of various thickness.

The conversion efficiency vs. θ_{RMS} is shown in Figure II-2.

II-3. Emittance Growth

The emittance growth of a beam due to scattering in a stripping foil during multiturn charge exchange injection has been discussed theoretically by Cooper and Lawrence⁽⁵⁾. For a normally distributed beam in transverse phase space the change in the emittance $\Delta\epsilon_N$ of the circulating beam after N injected turns is given by

$$\Delta\epsilon_N = \frac{\pi}{2} \beta_0 \cdot N \cdot nx [\sigma_c \langle \delta\theta^2 \rangle]$$

where β_0 is the value of the β function of the machine at the injection point, x is the foil thickness, and the quantity in brackets is the product of the effective Coulomb cross section for a collision and the mean square of a component of the angle caused by such a collision. The product of nx and the quantity in brackets is θ_{RMS} .

To obtain the numerical value of $nx [\sigma_c \langle \delta\theta^2 \rangle]$. We take $x = 100 \mu\text{g}/\text{cm}^2$.

$$\begin{aligned} nx &= x (\mu\text{g}/\text{cm}^2) \cdot \rho (\text{g}/\text{cm}^3) \cdot \frac{1 \text{ mole}}{A(\text{g})} \cdot 6.023 \frac{\text{atoms}}{\text{mole}} \times 10^{23} \\ &= 5.02 \times 10^{22} \frac{\text{atoms}}{\text{m}^2} \end{aligned}$$

$$\text{and } \sigma_c \langle \delta\theta^2 \rangle = \frac{\pi}{2} \left(\frac{Z \gamma_p E_0}{T} \right)^2 \left[\ln \frac{\theta_{\max}^2}{\chi_\gamma^2} - 1 \right] \quad (\text{II-3})$$

$$\text{where }^{(6)} Z=6 \quad E_0 = 938.26 \text{ MeV} \quad T= 93 \text{ MeV} \quad \beta = \frac{v}{c} = 0.415.$$

$$\gamma_p = \frac{e^2}{4\pi\epsilon_0 m_p c^2} = 1.5 \times 10^{-18} \text{ m}$$

$$\begin{aligned} \chi_\gamma &= 1.20 \theta_{\min} (1 + 3.33 \gamma^2)^{1/2} \quad \gamma = \frac{Z}{137} = 0.106 \\ &= 1.20 \times 1.019 \theta_{\min} \end{aligned}$$

$$\theta_{\min} = \frac{\hbar/p}{5.3 \times 10^{-11} Z^{-1/3} (\text{m})} = 1.58 \times 10^{-5} \text{ rad}$$

Now the question is how to calculate θ_{\max} . Where θ_{\max} is the maximum scattering angle that enters in equation (II-3).

$$\theta_{\max} = \frac{t_{1/p}}{1.6 \times 10^{-15} A^{1/3}}$$

In our case (Carbon $A = 12$) $\theta_{\max} = 0.126$ rad. with this value in formula (II-3) we get:

$$\sigma_c < \overline{\delta\theta^2} > = 21.45 \times 10^{-32} \text{ m}^2 \text{ rad}^2/\text{atom}$$

$$n \times \sigma_c < \overline{\delta\theta^2} > = 107.7 \times 10^{-15}$$

Take $N = 1$ and at injection point $\beta_s = 7$ m so

$$\Delta\epsilon_N = 0.038 \pi \text{ mm-mrad/turn}$$

For 60 turns ($N=60$) the beam emittance growth is 2.28π mm-mrad. And the resultant emittance is 12.28π mm-mrad. But the machine acceptance is 40π mm-mrad vertically and 92π mm-mrad horizontally. It means the acceptance has not been filled by multiple scattering effects.

E. Courant has suggested that a different θ_{\max} should be used⁽⁶⁾. Because θ_{\max} ($=0.126$ rad) is much bigger than the angle given by the machine's acceptance, particles will be lost and do not remain in the machine to contribute to the emittance growth. In the BPS Booster the maximum angles are 7.0 mrad vertically and 4.6 mrad horizontally at the injection point, with these values of θ_{\max} we get:

$$\sigma_c < \overline{\delta\theta^2} >_v = 12.87 \times 10^{-32} \text{ m}^2 \text{ rad}^2/\text{atom}$$

$$\Delta\epsilon_v = 0.014 \pi \text{ mm-mrad for } N = 1$$

$$\sigma_c < \overline{\delta\theta^2} >_h = 13.97 \times 10^{-32} \text{ m}^2 \text{ rad}^2/\text{atom}$$

$$\Delta\epsilon_h = 0.026 \pi \text{ mm-mrad for } N = 1$$

From this viewpoint the emittance growth is even smaller. In either case the emittance growth by multiple scattering is very slow. Particle losses will probably not result from multiple scattering, provided the beam does not remain on the foil beyond the time required for injection.

But if the acceptance has been filled by any other way. For example space charge effect, beam sweeping etc. Then particle losses could result from multiple scattering in the foil. Suppose that after the acceptance is filled the emittance growths are $\Delta\epsilon_v$ vertically and $\Delta\epsilon_h$ horizontally. Then for the relative growths:

$$\frac{\Delta\epsilon_v}{A_v} = \frac{\beta_v}{A_v} N \langle \overline{\theta^2} \rangle_v$$

$$\frac{\Delta\epsilon_h}{A_h} = \frac{\beta_h}{A_h} N \langle \overline{\theta^2} \rangle_h$$

Where A_v is the machine's acceptance, β_v the machine's β function and $\langle \overline{\theta^2} \rangle_v$ the RMS multiple scattering angle vertically and $A_h, \beta_h, \langle \overline{\theta^2} \rangle_h$, horizontally. N is the number of the particles in the machine.

The BPS Booster vertical acceptance is 40 π mm-mrad. Suppose the orbit bump fall time is 30 μ s (30 turns). According to the formulas above for $N = 30$ turns, the emittance growth is 1.14 π mm-mrad resulting in a fraction of particles lost of $1.14/40 = 3\%$, vertically first.

11-4. Circulating Beam Lifetime and "Orbit-bump" Fall Time

At the FNAL Booster, during DC operation at 200 MeV, the circulating beam intensity decays approximately exponentially to $1/e$ of the injected intensity at about $900 \mu s$ ($= 300$ turns) if allowed to remain on a foil of thickness $200 \mu g/cm^2$ (7). The beam lifetime being about 10 times longer with the foil removed. The "orbit-bump" fall time determines the length of time that the beam remains on the foil beyond injection. The FNAL design has a fall time of $30 \mu s$ ($= 10$ turns) for beam loss of the order of 3%. We will attempt to scale the lifetime of the Fermilab Booster beam to the BPS Booster.

According to the foregoing discussion on emittance growth,

we define the total losses as $\frac{\Delta \epsilon_v}{A_v} \cdot \frac{\Delta \epsilon_h}{A_h}$. We imposed the condition that:

$$\left. \frac{\Delta \epsilon_v}{A_v} \frac{\Delta \epsilon_h}{A_h} \right|_{\text{FNAL}} = \left. \frac{\Delta \epsilon_v}{A_v} \frac{\Delta \epsilon_h}{A_h} \right|_{\text{BPS}}$$

Then

$$\begin{aligned} & \left| \frac{\beta_v}{A_v} \frac{\beta_h}{A_h} \right|_{\text{FNAL}} \cdot N_F^2 \cdot \left| \langle \overline{\theta^2} \rangle_v \langle \overline{\theta^2} \rangle_h \right|_{\text{FNAL}} = \\ & = \left| \frac{\beta_v}{A_v} \frac{\beta_h}{A_h} \right|_{\text{BPS}} \cdot N_B^2 \cdot \left| \langle \overline{\theta^2} \rangle_v \langle \overline{\theta^2} \rangle_h \right|_{\text{BPS}} \end{aligned}$$

Where N_B will be the BPS Booster beam life-time and N_F is the FNAL Booster beam life-time, expressed in number of turns. We obtain:

$$\frac{N_B}{N_V} = \frac{(\sqrt{A_V A_h})_{\text{BPS}} (\sqrt{\beta_v \beta_h})_{\text{FNAL}} (\sqrt{\langle \bar{\theta}^2 \rangle_v \langle \bar{\theta}^2 \rangle_h})_{\text{FNAL}}}{(\sqrt{A_V A_h})_{\text{FNAL}} (\sqrt{\beta_v \beta_h})_{\text{BPS}} (\sqrt{\langle \bar{\theta}^2 \rangle_v \langle \bar{\theta}^2 \rangle_h})_{\text{BPS}}}$$

For the following numerical results:

BPS		FNAL	
$\gamma_v = 0.510 \text{ m}^{-1}$	$\gamma_h = 0.505 \text{ m}^{-1}$	$\gamma_v = 0.058 \text{ m}^{-1}$	$\gamma_h = 0.163 \text{ m}^{-1}$
$A_v = 40 \text{ } \mu\text{mm-mrad}$	$A_h = 92 \text{ } \mu\text{mm-mrad}$	$A_v = 16 \text{ } \mu\text{mm-mrad}$	$A_h = 25 \text{ } \mu\text{mm-mrad}$
$\beta_v = 4.23 \text{ m}$	$\beta_h = 6.94 \text{ m}$	$\beta_v = \frac{1}{\gamma_v}$	$\beta_h = \frac{1}{\gamma_h}$
$\langle \bar{\theta}^2 \rangle_v = nx \cdot 12.87 \cdot 10^{-32} \text{ m}^2 \text{ rad}^2 / \text{atom}$			BPS
$\langle \bar{\theta}^2 \rangle_h = nx \cdot 13.97 \cdot 10^{-32} \text{ m}^2 \text{ rad}^2 / \text{atom}$			BPS
$\langle \bar{\theta}^2 \rangle_v = nx \cdot 2.21 \cdot 10^{-32} \text{ m}^2 \text{ rad}^2 / \text{atom}$			FNAL
$\langle \bar{\theta}^2 \rangle_h = nx \cdot 2.68 \cdot 10^{-32} \text{ m}^2 \text{ rad}^2 / \text{atom}$			FNAL

$$x_F = 200 \mu\text{g}/\text{cm}^2.$$

We then obtain:

$$\frac{N_{\text{BPS}}}{N_{\text{FNAL}}} = \frac{208.5}{x_{\text{BPS}}}$$

that for $N_F = 300$ turns yields:

x_B ($\mu\text{g}/\text{cm}^2$)	N_B	τ_{fall}
40	1563.8	52.13 μs
60	1042.5	34.75 μs
70	893.6	29.79 μs
80	781.9	26.06 μs
100	625.5	20.85 μs

Shorter "orbit-bump" fall times are more difficult to obtain due to the requirements imposed on the fast pulsed magnets and their power supply. Thicker foils are easier to manufacture on the large sizes required. As a compromise we choose a foil thickness of $70 \mu\text{g}/\text{cm}^2$ with a fall time requirement of $30 \mu\text{s}$. And according to the calculation above for this thickness of foil the conversion efficiency is 99%.

II-5. Momentum Loss in the Foil

For a 93 MeV H^- traversing a Carbon foil the energy loss⁽⁴⁾ is:

$$\frac{dE}{dx} \approx 7 \times 10^{-6} \text{ MeV cm}^2/\mu\text{g}$$

then

$$\begin{aligned}\frac{\Delta P}{P} &\approx \frac{1}{2} \frac{1}{E} \left(\frac{dE}{dx} \right) x \\ &= \frac{1}{2 \cdot 93 \text{ MeV}} (7 \cdot 10^{-6} \text{ MeV cm}^2 / \mu\text{g} \cdot x) \\ &= 3.76 \cdot 10^{-8} x\end{aligned}$$

$$\begin{aligned}x &= 40 \mu\text{g/cm}^2 \\ &60 \mu\text{g/cm}^2 \\ &80 \mu\text{g/cm}^2 \\ &100 \mu\text{g/cm}^2\end{aligned}$$

$$\begin{aligned}\frac{\Delta P}{P} &= 1.5 \times 10^{-6} \\ &2.3 \times 10^{-6} \\ &3.0 \times 10^{-6} \\ &3.7 \times 10^{-6}\end{aligned}$$

For H^- traversing a $70 \mu\text{g/cm}^2$ foil 60 turns, the momentum loss is $\Delta P/P = 2.6 \times 10^{-6}/\text{turn} \times 60 \text{ turns} = 1.56 \times 10^{-4}$. The BPS Booster machine $\Delta P/P$ acceptance at injection is 2×10^{-3} . Thus the momentum loss in the foil is not expected to result in losses.

II-6. Stripping Foil Life Time

Under ion bombardment the foil life time is a function of the energy loss on the foil per unit volume. In Reference⁽⁸⁾ a compendium of experimental results can be found. The foil life time does not seem to depend on the foil thickness. The foil life time in the low energy range is given by the empirical formula:

$$\tau(p, \mu\text{A} \cdot \text{min/mm}^2) = 20 \cdot E^{1.15} (\text{MeV/amu})$$

For our case, the conditions are energy = 93 MeV, and H^- beam bombarding area of 220 mm^2 , a duty cycle of 12.5 p/s

with an intensity of 5×10^{12} ppp. For our injected turns of 30 and a fall time of $30 \mu\text{s}$ the number of particles traversing the foil is:

$(30 + 29 + 28 + \dots + 3 + 2 + 1) + 30 = 495$ times the injected number. We obtain:

$$\begin{aligned}\tau &= 3671 \text{ (p.}\mu\text{A} \cdot \text{min/mm}^2\text{)} \\ &= 3.671 \times 10^3 \times 60 \times 220 \times 10^{-6} / 1.602 \times 10^{-19} \\ &= 3.1 \times 10^{20} \text{ particles.}\end{aligned}$$

So the foil life time is

$$\frac{3.1 \times 10^{20}}{\frac{5 \times 10^{12} \times 12.5}{30} \times 495} = 4 \text{ days}$$

An independent way of estimating the foil life time is to scale to the BPS Booster from the FNAL Booster. At FNAL more than one year foil exposures have been achieved.

The foil life time is inversely proportional to the energy loss on the foil, the number of particles, the number of foil traverses, and the accelerator duty cycle, and it is proportional to the bombarding area. Suppose the BPS Booster foil life time is τ_B and for FNAL Booster foil life time $\tau_F = 1$ year.

Then:

$$\tau_B = \tau_F \frac{\left(\frac{dE}{dx}\right)_F \left(\frac{\text{total inj - parti.number}}{\text{injection turns}} \cdot \text{through foil times} \right)_{\text{FNAL}}}{\left(\frac{dE}{dx}\right)_B \left(\frac{\text{total inj - parti.number}}{\text{injection turns}} \cdot \text{through foil times} \right)_{\text{BPS}}}$$

$$\times \frac{(\text{Booster duty cycle Main ring duty cycle})_{\text{FNAL}}}{(\text{Booster duty cycle Main ring duty cycle})_{\text{BPS}}}$$

$$\times \frac{(\text{Bombarding area})_{\text{BPS}}}{(\text{Bombarding area})_{\text{FNAL}}}$$

$$= 1 \text{ year} \cdot \frac{4 \times 10^{-3} \text{ MeV/mg/cm}^2}{7 \times 10^{-3} \text{ MeV/gm/cm}^2} \cdot \frac{2 \times 10^{12}}{6} \cdot (6+5+4+3+2+1) \cdot \frac{13}{(s)} \cdot \frac{1}{10(s)} \\ \cdot \frac{3 \times 10^{12}}{30} \cdot 495 \cdot \frac{12.5}{(s)} \cdot \frac{1}{5(s)}$$

$$\times \frac{220 \text{ mm}^2}{380 \text{ mm}^2} = 6 \text{ days.}$$

This result is a minimum, as no foil at FNAL has failed due to beam exposure, and it is in good qualitative agreement with the previous estimate of 4 days.

II-7.Foil Size

A diagram of the BPS Booster H^- injection system is shown in Fig. I-2. The 93 MeV H^- ions from a linear accelerator pass through a Carbon stripping foil at the injection point. The electrons are stripped off the H^- ions by the foil and the resulting beam of protons is set in the accelerator closed orbit by the orbump magnets MBHI₃ and MBHI₄. The H^- cross-section is 2.2 cm^2 . The maximum circulating beam cross-section is 16.64 cm^2 . The dimensions of the free area of the stripping foil must be large enough so that no circulating beam can strike the foil holder. The "C" shaped frame with the dimension indicated in Fig. II-3 is utilized for mounting the foils. The unsupported area of the mounted foil is about 27 cm^2 . To reduce the emittance growth due to multiple scattering, the circulating beam is moved off the foil after injection is completed. The free edge of the foil provides an obstruction free path for the beam to move across.

II-8.Foil Holder

The foil life time is about 4-6 days. If we will need to change foils on the order of once a week there should be some spare foils within the vacuum chamber for easy exchange. The foils could be mounted on a manipulator of the type of the FNAL Booster. A large storage capacity can be obtained in a small space as well as large separation for the foil in use. It should be easy to store in the order of 20 foils without complicated mechanical design. The FNAL's design is very useful for our reference.

References:

- 1) H. Tawara and A. Russek, Rev. Mod. Phys. 45 178, 1973.
- 2) C. Hojvat, M. Joy, R.C. Webber, IEEE NS-26 p. 4009 1979.
- 3) R.C. Webber and C. Hojvat, IEEE NS-26 p. 4012, 1979.
- 4) M. Joy, FNAL TM-699, November 22, 1976.
- 5) R.K. Cooper and G.P. Lawrence, IEEE NS-22 p. 1916, 1975.
- 6) E.D. Courant, R.S.I. 24 No. 9, p. 836 1953.
- 7) C. Hojvat, private communication.
- 8) A.E. Livingston, H.G. Berry and G.E. Thomas, N.I.M. 148 p. 125 1978.

TABLE II-1

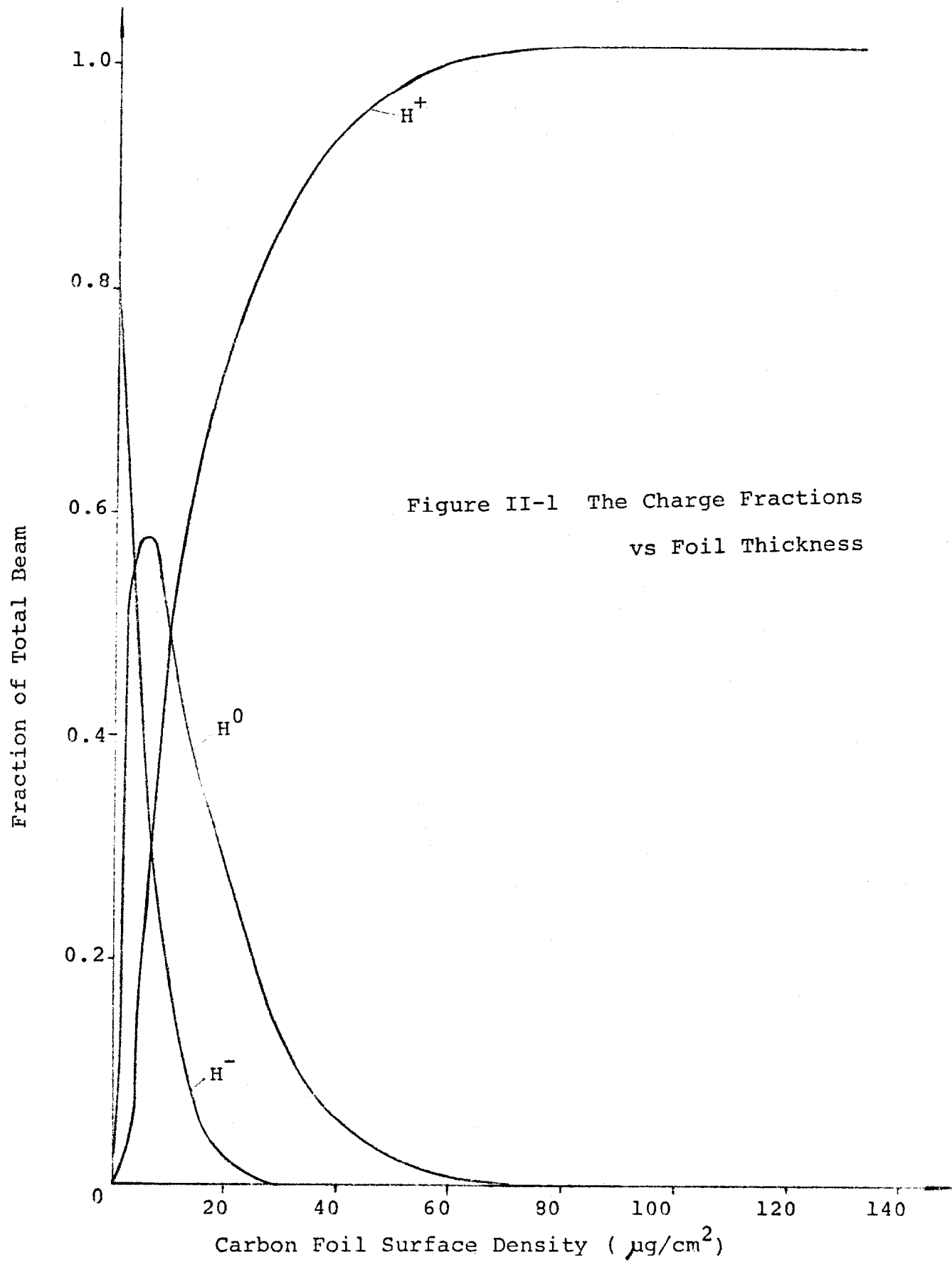
BEAM FRACTIONS N^- , N^0 , N^+ AS A FUNCTION
OF THE THICKNESS OF THE CARBON FOILS

$x(\text{ g/cm}^2)$	$n(\text{atoms/cm}^2 \times 10^{18})$	N^-	N^0	N^+
2	0.10	0.67	0.31	0.025
5	0.25	0.37	0.51	0.12
8	0.40	0.20	0.57	0.23
10	0.50	0.13	0.54	0.33
15	0.75	0.049	0.44	0.51
20	1.0	0.018	0.33	0.66
40	2.0	3.2×10^{-4}	0.078	0.92
60	3.0	5.9×10^{-6}	0.017	0.98
80	4.0	1.06×10^{-7}	3.9×10^{-3}	0.996
100	5.0	~ 0	8.6×10^{-4}	0.999

TABLE II-2

THE RELATION OF THE CONVERSION EFFICIENCY
AND θ_{RMS} FOR CARBON FOILS OF
VARIOUS THICKNESS

x ($\mu\text{g}/\text{cm}^2$)	$\langle \overline{\theta^2} \rangle^{1/2}$ (rad)	N^+
5	2.8×10^{-5}	0.12
10	4.1×10^{-5}	0.33
20	5.8×10^{-5}	0.66
40	8.2×10^{-5}	0.92
60	10.0×10^{-5}	0.98
80	11.5×10^{-5}	0.996
100	12.9×10^{-5}	0.999



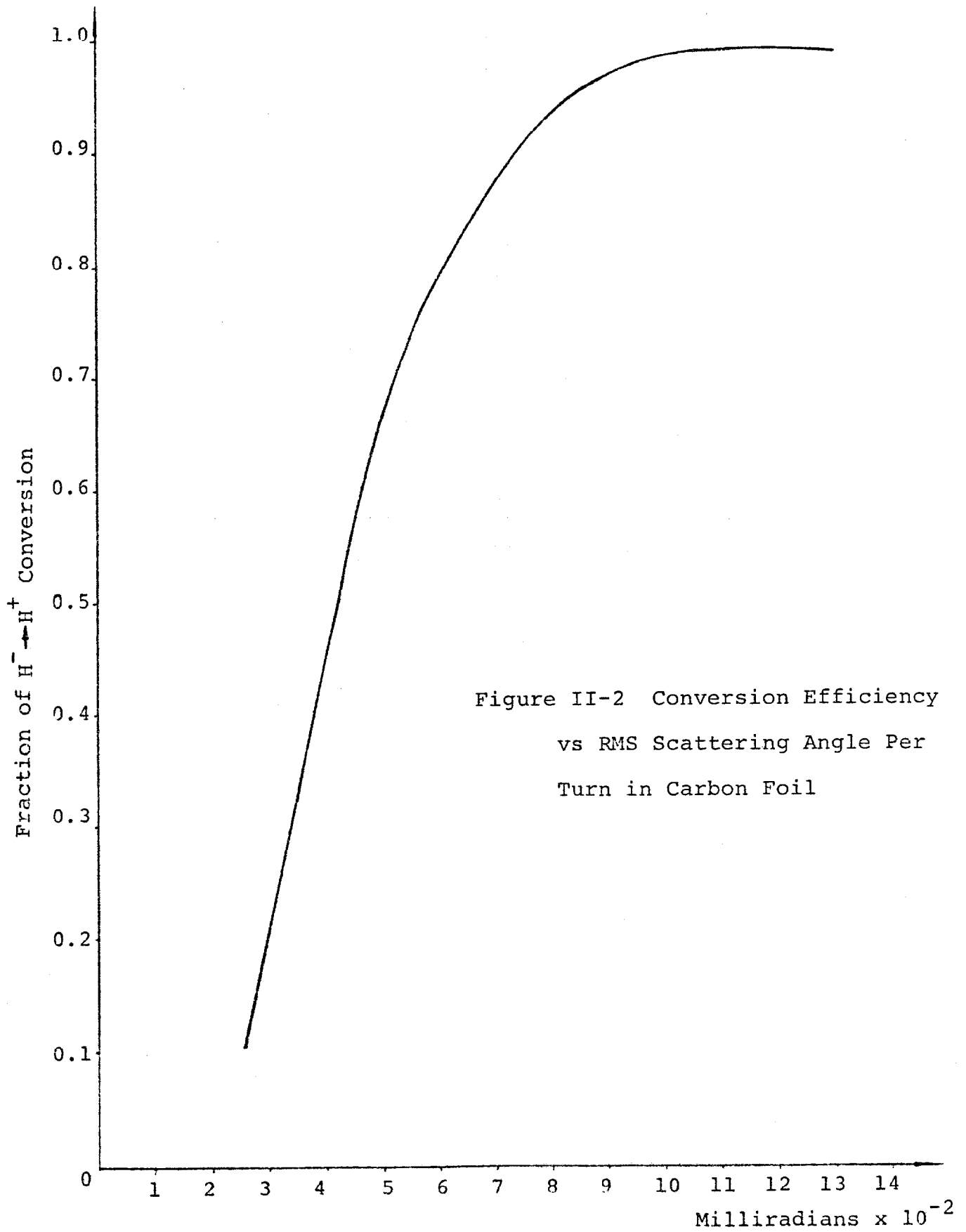


Figure II-2 Conversion Efficiency
vs RMS Scattering Angle Per
Turn in Carbon Foil

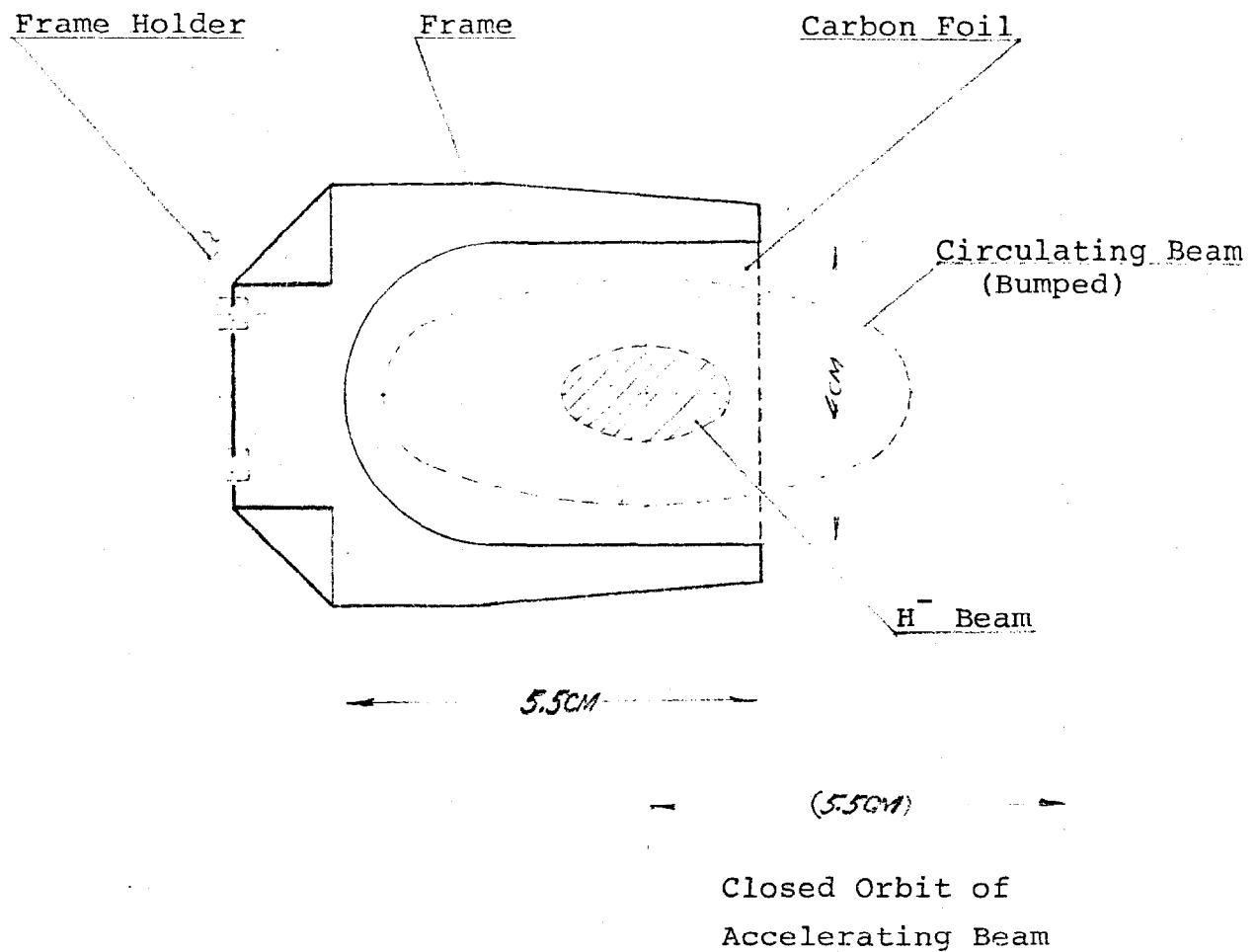


Figure II- 3 Foil Frame

CHAPTER III (a)

THE ORBUMP MAGNETS FOR BOOSTER INJECTION

Y.S. Shi

III-1 Introduction

For simplicity, the four orbump magnets of the H^- injection into the Beijing Booster are identical and separated. Their windings can be connected electrically in a parallel-series configuration. It is necessary to have the four orbump fields tracking simultaneously to prevent orbit distortion during injection. It also simplifies the fabrication and provision for spares. Because the four magnets are separated, the required deflection can be obtained at lower fields with less strain on the power supply and magnet insulation. To achieve this advantage, the long straight section was increased by 0.3 meters.

To determine the dimensions of the orbump the following parameters are required:

Core length	40 cm
Pole width	17 cm
Gap between poles	5.6 cm
Maximum flux density in the gap	2804 gauss

III-2 Yoke Design

The orbump magnets should be made of Peoples Republic of China (PRC) materials. We do not have the specifications of silicon-iron electrical steels. At present, we are using MAGESIL-N steel specifications in this design and will make appropriate corrections for the use of PRC steel.

The core structure is a window frame type. The opening is 19 cm in width and 5.6 cm in height. The frame width is 6 cm all around. The thickness of the laminations is 0.2 mm (0.008") which was determined after a comparison among 0.10, 0.15, and 0.20 mm thicknesses. Although the 0.15 mm thickness is suitable and 0.10 mm even better, the 0.20 mm thickness (also suitable for our requirement), was chosen because sizes less than this are available only upon special order in the PRC. See figure III-1.

The maximum flux density in the laminations, B_{\max} , is $2804 \times (17/2 \times 6) \times (1/0.9) = 4414$ gauss.

The stacking factor of laminations for the epoxy molded core can have a mean value of 0.9 in the calculations for core losses we take $B_{\max} = 4500$ gauss. The magnetizing current of the core, I_{\max} , will be $0.2804 \times 0.056 / (4\pi \times 10^{-7}) = 12500$ amp.

The magnetizing force of the iron is neglected, for 0.007" MAGNESIL-N steel at an induction level of 4500 gauss the magnetizing force is about 0.8 oersted requiring an exciting current less than 25 amp or 0.2% of the total.

The orbump magnet carrying a current pulse with a falling time of a few tenths of microseconds produces the required pulsed magnetic field during H^- injection. The core losses and the effective skin depth at different falling rates are calculated as follows.

The typical waveform of the exciting current pulse is shown in Figure III-2, t_f - fall-time - is the time required to shut down the orbump, t_t is the flat-top of the pulse for injection, t_r - the rise-time - is the time required to build up the peak exciting current, and t_i is the time required to reach the peak at the maximum rate of rise of the exciting current.

In general, we have the relations between t_f , t_r , and t_i as follows

$$t_f = 1.2 t_r \qquad t_i = 0.7 t_r$$

The total duration of a pulse would be $t_r + t_t + t_f$. The repetition rate of 12.5 times per second is determined by the booster operation.

Eddy current shielding causes the flux near the middle of the magnetic specimen to lag behind the flux at the surface and to produce a nonhomogeneous induction. At a given frequency such a lag will cause the permeability to be substantially below that measured. From the chart of MAGNESIL-N 0.007" thick lamination the ac permeability μ_r at different frequencies vs induction takes the values as follows:

t_f	(μs)	20	30	40	50	60	100
t_r	(μs)	16.7	25	33.3	41.7	50	83.3
t_i	(μs)	11.7	17.5	23.3	29.2	35	58.3
$f_i (=1/4t_i)$	(kHz)	21.4	14.3	10.7	8.56	7.14	4.29
$\mu_r (B_{max}=4500 \text{ g})$		1200	1600	2000	2500	3000	5000
$t_i \mu_r \times 10^7$		2.57	2.29	2.14	2.14	2.14	2.14

Note that the permeability is strongly dependent on the frequency up to around 10 kHz. Above that frequency, the permeability decreases to some extent with increase in frequency, but this effect is not strong.

The effective skin depth, d , holds a relation with the resistivity ρ_i , the frequency f_i , and the permeability μ , as $d = \rho_i / \pi f_i \mu$, where $\rho_i = 48 \times 10^{-8} \text{ ohm-m}$.

We obtain:

t_i	(μs)	20	30	40	50	60	100
d	(mm)	0.070	0.073	0.076	0.076	0.076	0.076
$2d$	(mm)	0.14	0.15	0.15	0.15	0.15	0.15

It shows that the suitable thickness, $2d$, of lamination is 0.15 mm thick. There is a possibility to choose the 0.20 mm thick instead of 0.15 mm thick, because the actual flux density is lower and the permeability may be much lower for our ordinary electrical steels. If the value of μ_r reduces

to 1200 at 14.3 kHz (i.e., assuming the μ_r holds constant at 21.4 kHz), then the effective skin depth will be

t_f	(μs)	20	30	(40)
d	(mm)	0.070	0.085	(0.098)
2d	(mm)	0.14	0.17	(0.20)

Thus if some core losses are permissible, we may elect to make the magnet of 0.20 mm sheets, which is advantageous for utilizing PRC steel.

The core losses, P, is comprised of two parts, one is hysteresis loss P_h , the other is eddy current loss P_e . The harmonic components of the pulsing flux causes increases in core loss, but we do not consider it to be important in our engineering estimation.

The data for core loss of MAGNESIL-N is not shown above 400 gauss at 20 kHz, nor above 1000 gauss at 10 kHz. We can determine it at two different frequencies by extrapolation when the flux density is moderate. The permeability of this material is much reduced at higher frequency. The effective permeability is also considerably reduced due to the existence of joints and gaps in the magnetic circuit. So the calculation only gives an approximation.

The hysteresis loss P_h may be expressed as $P_h = k_h B_{max}^{1.6} f$ watts per unit weight, where k_h is the hysteresis loss constant and f is the exciting current frequency, B_{max} is the maximum flux density in the core.

The eddy current loss P_e is $P_e = k_e B_{max}^2 \cdot f^2$ watts per unit weight, where B_{max} , f are the same as above, k_e is the eddy current loss constant but it is a function of the lamination thickness.

The MAGNESIL-N 0.007" thick laminations have a typical loss characteristic at $B_{\max} = 1000$ gauss as

$$f = 200 \text{ Hz} \quad ; \quad P = P_h + P_e = 0.042 \text{ watt/lb}$$

$$f = 1000 \text{ Hz} \quad ; \quad P = P_h + P_e = 9.0 \text{ watts/lb}$$

$$\text{i.e., } k_h \times (1000)^{1.6} \cdot 200 + k_e \cdot (1000)^2 \cdot 200^2 = 0.042$$

$$k_h \times (1000)^{1.6} \cdot 10000 + k_e \cdot (10000)^2 \cdot 100000^2 = 9.0$$

From above, we get:

$$k_e = 7.04 \times 10^{-14} \quad ; \quad k_h = 3.10 \times 10^{-9}$$

For $B_{\max} = 4500$ gauss and 0.007" thick laminations to simplify the calculation at different current falling rates, the core losses will be

$$\begin{aligned} P_h &= k_h \times (4500)^{1.6} \times 12.5 \\ &= 3.10 \times 10^{-9} \times 7.0 \times 10^5 \\ &= 2.71 \times 10^{-2} \text{ watts/lb} \end{aligned}$$

$$P_e = k_e \times (4500)^2 \times f^2 \text{ watts/lb}$$

$$\text{or, } P_e = k_e \times (4500)^2 \times f \text{ watts per lb per cycle}$$

Note that the current pulse is not sinusoidal. However the rising and the falling portions are considered as sinusoidal. The eddy current loss for the rising portion of the pulse is $k_e \cdot (4500)^2 \cdot f_r^2 \cdot (12.5/4f_r)$, where the factor in the bracket $(12.5/4f_r)$ is the duty factor. Likewise the falling portion of the pulse produces a loss due to eddy current effect $k_e \cdot (4500)^2 \cdot f_f^2 \cdot (12.5/4f_f)$. The total eddy current loss would then be:

$$\begin{aligned}
 P_e &= k_e \cdot (4500)^2 \cdot (f_r + f_f) \cdot 12.5/4 = \\
 &= 7.04 \cdot 10^{-14} \cdot 2.03 \cdot 10^7 \cdot 3.13 \times (f_r + f_r) = (\text{watts/lb}) \\
 &= 4.46 \cdot 10^{-6} (f_r + f_r) \quad (\text{watts/lb})
 \end{aligned}$$

Scaled from 0.007" to 0.20 mm by the square of the thickness ratio 1.265, so that:

$$P_e = 5.64 \cdot 10^{-6} (f_r + f_f) \quad (\text{watts/lb})$$

t_f	(μs)	20	30	40	50	60	100
$t_f (=1/4t_f)$	(kHz)	12.5	8.33	6.25	5.0	4.17	2.5
$f_r (=1/4t_r)$	(kHz)	15.0	10.0	7.5	6.0	5.0	3.0
$f_r + f_r$	(kHz)	27.5	18.33	13.75	11.0	9.17	5.5
P_e	(mw/lb)	155.2	103.4	77.6	62.0	51.7	31.0

The core weight is $(31 \times 17.6 - 19 \times 5.6) \times 40 \times 7.65 \times 0.9 = 121000$ grams, or 266.8 lb.

The total core loss and the heat generated in the iron core at different falling rates would be:

t_f	(μs)	20	30	40	50	60	100
$p (=P_e + P_h)$	(mw/lb)	182.3	130.5	104.7	89.1	78.8	58.1
	(watts)	48.6	34.8	27.9	23.8	21.0	15.5
Q	(cal/sec)	11.7	8.4	6.7	5.7	5.0	3.7

About 20 kcal. of heat will cause a temperature rise of 1 deg centigrade in the core, the calculated core loss is very small so it is negligible for the temperature rise.

III-3 Coil Design

The effective skin depth of the copper conductor at frequency f_i will be:

t_f	(μs)	20	30	40	50	60	100
d	(mm)	4.51	5.52	6.38	7.13	7.81	10.1
$2d$	(mm)	9.0	11.0	12.8	14.3	15.6	20.2

Note $d = \sqrt{\rho_{cu} / \pi f_i \mu_0} = 6.6 / \sqrt{f_i}$ cm; $\rho_{cu} = 1.724 \times 10^{-8}$ ohm-m;
 $\mu_0 = 4\pi \times 10^{-7}$.

If the conductor is made of OFHC 4 mm thick, we can ignore the skin effects, and the dc resistance may be considered as the ac resistance.

The copper winding, cross connections and feed-through leads have a cross sectional area of $50 \times 4 \text{ mm}^2$, and a total length of about 2 m. The resistance will be 1.724×10^{-4} ohm. The copper loss is given by:

$$[(I_{\max} / \sqrt{2})^2 t_r + I_{\max}^2 t_t + (I_{\max} / \sqrt{2})^2 t_f] \cdot 1.724 \times 10^{-4} \cdot 12.5 \text{ (watts)}$$

Where $I_{\max} = 12500$ amperes, the factor $1/\sqrt{2}$ is the effective coefficient of a sinusoidal wave, 12.5 is the number of pulses per second. For different falling rates and $t_t = 60 \mu s$, we have:

t_f	(μs)	20	30	40	50	60	100
P_{cu}	(watt)	27.0	29.5	32.6	35.6	38.7	51.1
Q_{cu}	(cal/sec)	6.62	7.08	7.82	8.54	9.29	12.3

The copper weighs about $200 \times 0.4 \times 5.0 \times 8.94 = 3576$ grams, and the specific heat at 25°C is $0.092 \text{ cal/g/}^{\circ}\text{C}$. The heat required for 1°C temperature rise without any dissipation is $0.092 \times 3576 \times 1 = 329 \text{ cal}$. The OFHC copper has a high thermal conductivity at 20°C as $0.934 \text{ cal/sq.cm/cm/sec/}^{\circ}\text{C}$. If the connecting surfaces of joints between the winding leads and the strip bus have sufficient contact area (say, $5 \times 5 \text{ cm}^2$) and lower contact resistance, the heat would transfer out of the winding then the temperature rise of the winding would not exceed 5 to 10°C or the rising rate of temperature will be 0.02°C/s to 0.037°C/s if the winding had perfect heat insulation.

III-4 Insulation Design

The self inductance of the winding is approximately

$$L = 4\pi \times 10^{-7} \times 0.17 \times 0.4 / 0.056 = 1.53 \times 10^{-6} \text{ henry}$$

The maximum voltage existing between the leads of the winding is

$$V = 1.53 \times 10^{-6} \times 12500 / (t_i \times 10^{-6}), \text{ we have}$$

t_F	(μs)	20	30	40	50	60	100
t_i	(μs)	11.7	17.5	23.3	29.2	35.0	58.3
V	(volts)	1632	1091	830	654	546	338

As the magnets are connected in series/parallel, the coil must float electrically, so the winding insulation should withstand a higher voltage, a minimum of 3000 volts. Furthermore, the yokes will be insulated from ground for double insulation.

A 5mm thick insulation on the coil is sufficient if made with glass cloth and molded with epoxy resin under vacuum, a layer of KAPTON putting under the winding gives a good insulation with the core.

III-5 Epoxies

The magnetic core potting to vacuum impregnation is submerged into an epoxy mixture which has the following ratio, parts by weight:

DER 332 75g; NMA 65g; DMP 30 1g

The copper winding potted with room-cure epoxy by the following ratio, parts by weight:

DER 332 100g; EM 308 80g

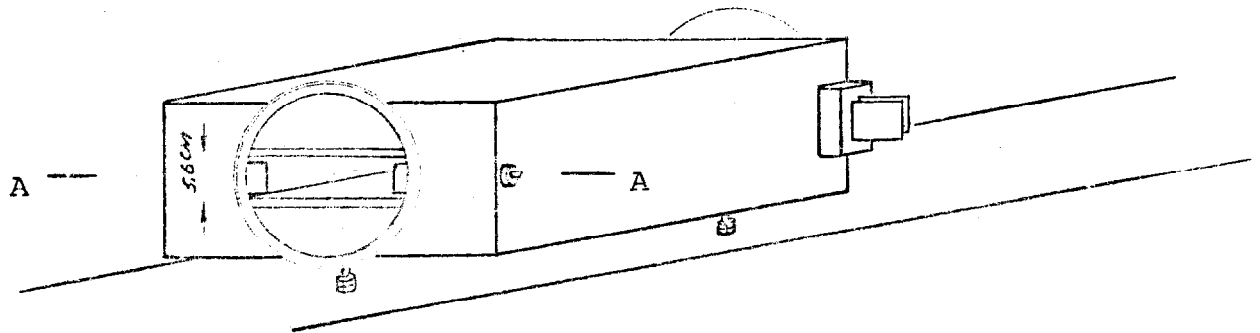
Any epoxy exhibiting outstanding properties of low viscosity, exceptional resistance to impact and thermal shock, eliminating microscopic cracking can be used for the molding purpose. A program to study Chinese epoxies should be started to determine if the above requirements could be met.

III-6 Mechanical Stress

A mechanical repulsive force is developed between the two conductors of the coil when a current flows. At peak current, there will be a compression total force of 140 kg existing on the epoxy insulation. Due to the large supporting area ($5 \times 40 = 200 \text{ cm}^2$), the maximum compressive stress on epoxy insulation is only about 0.7 kg/cm^2 . The insulation can easily withstand this load.

The pulsed current through the coil is unidirectional. Although the compressive force varies periodically, the molded insulation has only a small amount of compressive reflection.

Other requirements in detail are shown in the mechanical drawings.



Section A-A

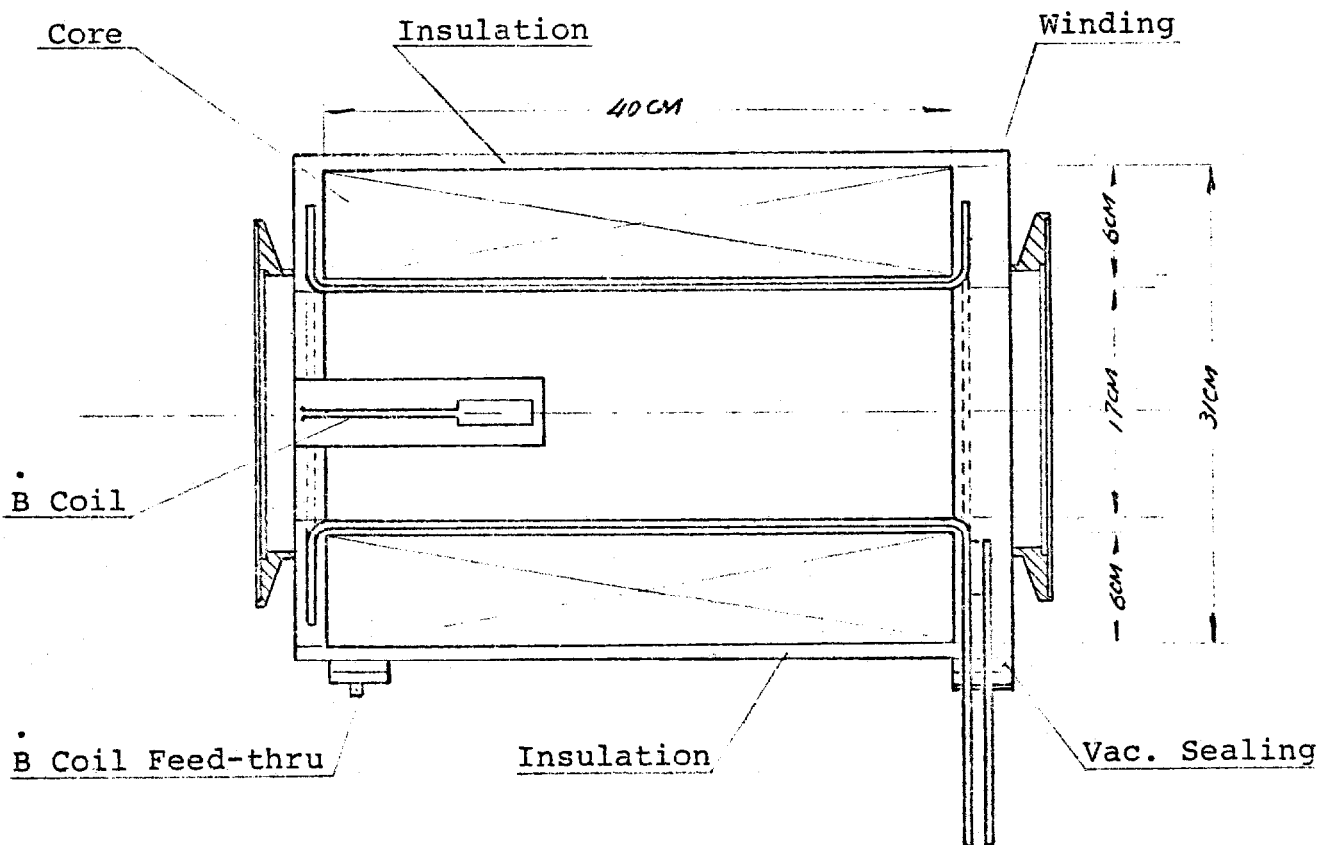


Figure III- 1 The Orbump Magnet

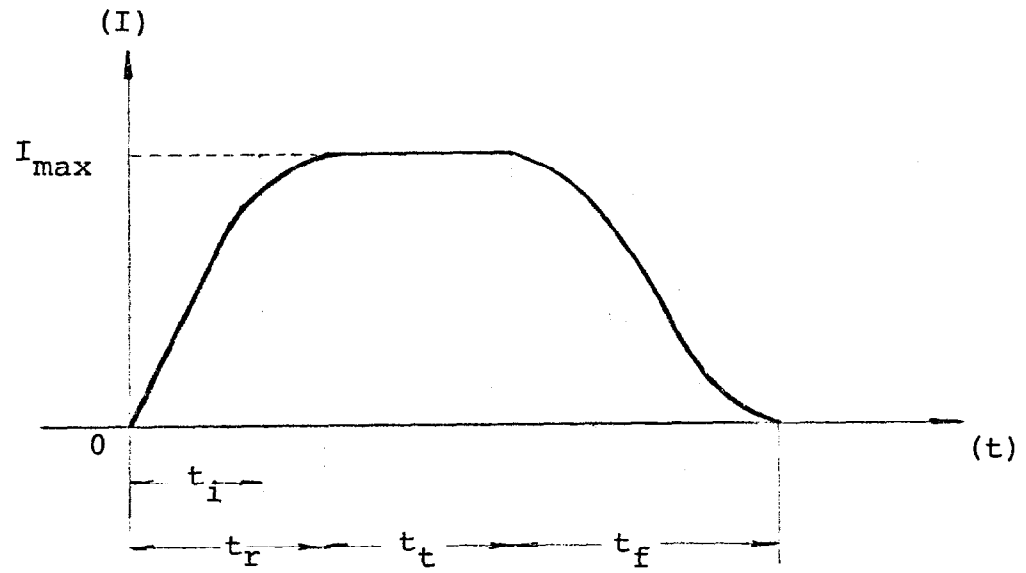


Figure III-2 Current Wave-form for Orbump Magnets

CHAPTER III (b)

THE SEPTUM MAGNET FOR BOOSTER INJECTION

Y.S. Shi

III-7 Introduction

In the Beijing Booster, injection takes place in a long straight. The 93 MeV beam transport line is located at 24.83° with respect to the long straight axis. The injected beam is bent by 24.83° in a septum magnet, emerging parallel to the closed orbit. The septum magnet has parameters as follows:

Deflection angle:	433.3 mrad
Magnetic field:	6874 gauss
Length:	0.9 m
Aperture:	40 mm H x 35 mm V
Injection time:	30 μ s
Fall time:	100 μ s (for pulsed power supply) or dc

There are two choices for the septum magnet, one is a pulsed septum magnet, the other is a dc magnet. For a pulsed septum magnet we must provide a 25 kA pulsed power supply and the magnet must be put in a vacuum box causing a difficulty with the compactness of the straight section. The space between the iron cores of the ring bending magnets and the injection septum magnet is only 15 cm, which is too short for the size of the bending magnet winding, and the septum magnet coil end, and the vacuum connections. Compared with a pulsed septum magnet, the dc septum magnet using a vacuum tube instead of a vacuum box makes the mechanical arrangement much easier, and a relatively small dc power supply of the order of 250 A, 35 V can be used instead of the 25 kA pulsed power supply. The economic advantage is obvious, if the problem of the fringing field on the circulating beam can be solved or reduced to a acceptable level. We describe here the design of such a dc septum magnet.

The curved core is stacked with laminations and welded together with a radius of curvature of 2077 mm in the center of the pole profile in coincidence with the center line of vacuum chamber. At the upstream and downstream ends we weld the wedge shaped end plate to make a monolithic sector core. Both the injecting and exiting beams are perpendicular to the end surfaces. The end plates have cuts to reduce the sextupole components. See figure III-3.

The core is mounted and welded on the base plate, in which a curved block is fastened as the reference during stacking the laminations. When the block is taken off, we fasten the manifolds of the cooling system and the electric connectors (in the recess of the core) on the base plate.

On the plain pole profiles there are ROSE SHIMS to improve the field distribution within the limit of 0.1% overshoot at 6874 gauss. The dimensions of the shim were calculated by Dr. S.C. Snowdon as

$$a=10.7 \text{ mm}, b=1.0 \text{ mm}; \text{ or } a=7.2 \text{ mm}, b=1.5 \text{ mm}$$

We choose the former. See Figure III-4.

The guards of the pole reduce the fringing magnetic fluxes considerably. Around the vacuum chamber of the circulating beam parallel, to the septum magnet at the downstream end, we mount two coaxial cylinders to make the magnetic shielding. Each cylinder is 1.5 mm thick and made of mild steel sheet. Between them there is an aluminum or stainless steel cylindrical spacer to separate the magnetic shields by 1.5 mm in distance. This length of the shield, 250 mm, is good enough. This shielding will reduce the magnetic field affecting the circulating beam by a factor of 10^{-3} .

The magnetic flux density at the core would be:

$$B_{\text{gap}} = 6874 \text{ gauss},$$

$$B_{\text{end of guard}} = 6874 \text{ gauss},$$

$$B_{\text{root of pole}} = 14470 \text{ gauss},$$

$$B_{\text{root of guard}} = 8020 \text{ gauss}.$$

The core is protected from rusting by painting, it does not require potting in epoxy. The magnetizing force is approximately 23700 ampere-turns.

III-9 Coil Design

The total excitation is 23700 amp-turns. We use 6 pancake type coils wound with hollow conductor of general electrical copper (not OFHC) 5.2 mm x 5.2 mm sq 3.6 mm diameter hole. The coil working on a relatively low voltage of 35 volts each has 5x7 turns wrapped with silaned fibre-glass tape, half lapped for insulation between adjacent turns and layers, the wrapped together and put it into potting fixture to impregnate with room temperature cured epoxy (same as the orbump coil). The final cross sectional area of coil is held within 30 mm height x40 mm width. Spacers are used to fix the coils in position.

The 6 coils are connected electrically in two branches, each branch has 3 coils in series. As for the cooling water system, all the coils are connected in parallel through two manifolds.

Each coil has a copper weight of 12.55 Kg (copper cross sectional area 16.8 mm^2 , conductor length 84 m) and its resistance is 0.086 ohm at 20°C, 0.103 ohm at 70°C.

III-10 Cooling

Each coil carries $23700/210 = 113$ amp. If the temperature rise is 50°C from the room temperature, it will generate a heat of

$$113^2 \times 0.103 \times 0.24 = 315 \text{ cal/sec.}$$

The conductor has a hole of 3.6 mm diameter. It passes cooling water 0.2 gal per min, i.e, 12.6 grams of water per second, the temperature rise of water would be $315/12.6 = 25^\circ\text{C}$. The cooling water just has a temperature rise half of the copper temperature rise. The flow rate is just satisfactory if the inlet temperature is 20°C.

The pressure drop is 93 m head per 100 m length at a flow rate 0.2 gal/min for copper conductor 0.14" (3.56 mm) diameter hole. So the pressure drop of the coil would be $84 \times 0.93 = 78.12$ m head (roughly 8 Kg/cm²). Considering the resistance in rubber hoses, manifolds and bends, 10 Kg/cm² pressure drop would be sufficient.

Cooling water consumption is 1.2 gal/min (72 gal/hr), or 273 Kg/hr. The amount is relatively small.

III-11 Power Supply

The necessary dc power supply is rated as:

Voltage:	35 V
Current:	226 A
Stability:	$\pm 0.1\%$
Rating:	Continuous

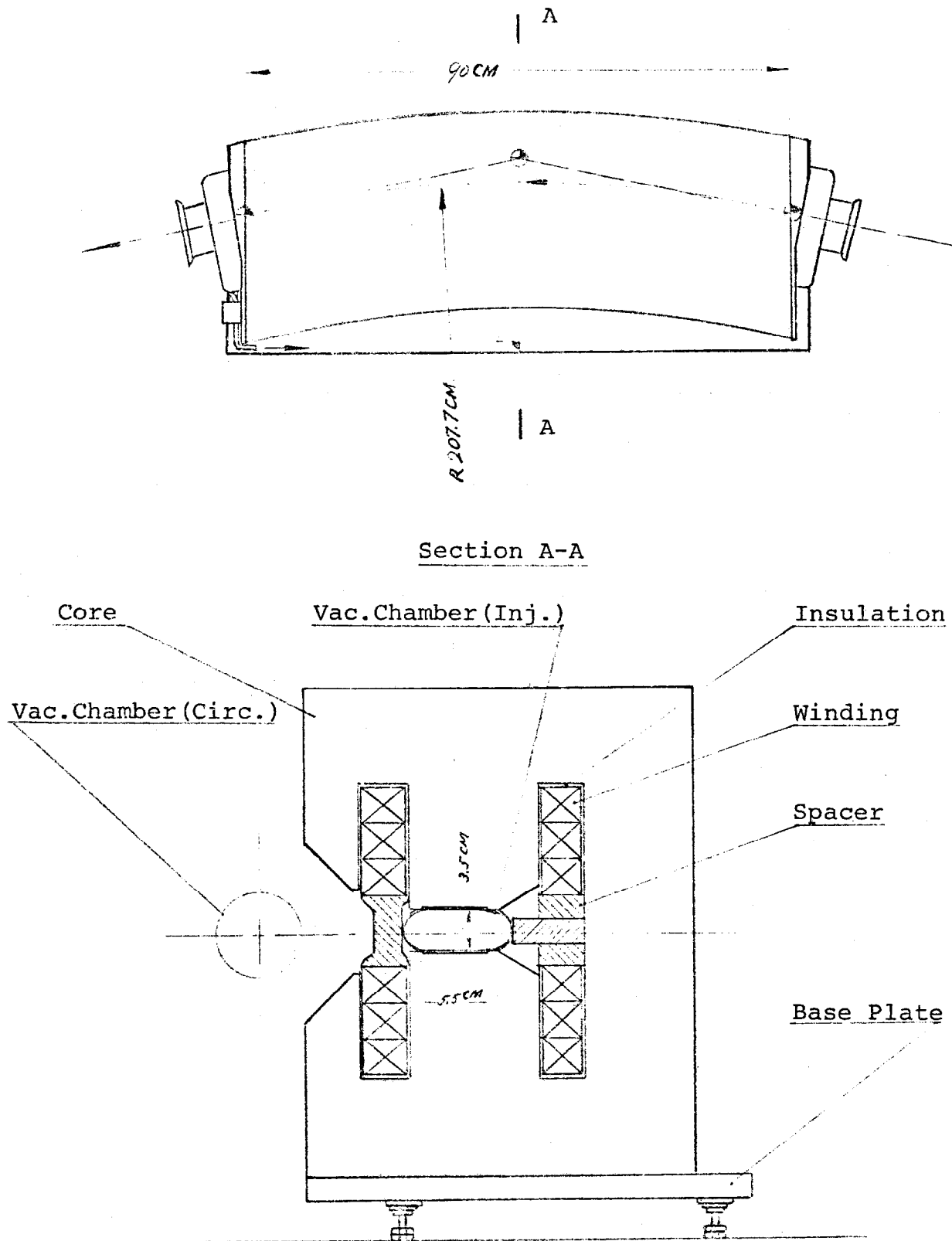


Figure III-3 The D.C. Injection Septum

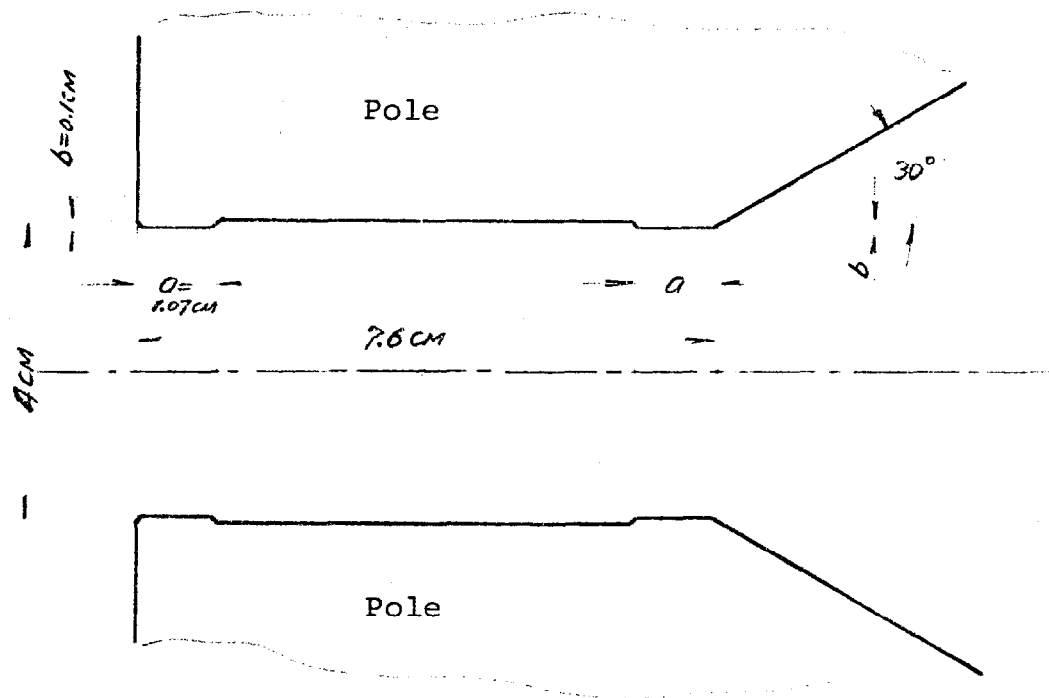


Figure III-4 Detail of the Injection Septum Rose Shims

Jiang Yan-Ling

IV-1. Introduction

The multiturn injection of H⁻ ions, adopted in the design of the Beijing Booster, requires the shifting of the closed orbit towards the injection trajectory so as to allow the circulating protons to overlap with the injected negative ions at the stripping foil. This can be accomplished utilizing an "Orbump" magnet, excited with a trapezoidal current pulse. The power supply, whose function is to provide this current pulse, must satisfy the following specifications:

load inductance	$L_m = 1.58 \mu\text{H/magnet}$
quantity of magnets	4
peak current	$I_p/\text{magnet} = 12.5 \text{ kA},$
duration of flattop of pulse	$60 \mu\text{s},$
fall time of pulse	$30 \mu\text{s},$
repetition rate	12.5 pps.

IV-2. Conceptual Design

Since the function of our "Orbump" power supply is almost the same as the one used at the Fermilab Booster and furthermore Fermilab's design has proven an excellent combination of reliability, cost and flexibility, we will adopt a similar concept (Fig. IV-1).

IV-3. Calculation of the Discharge Loop

According to the method suggested by Ken Bourkland, the parameters of the components in the discharge loop can be calculated as follows (Fig IV-2):

$$t_r = t_f/1.2 = 25 \mu\text{s},$$
$$f = 1/(4 \times 0.7t_r), = 14.285 \text{ kHz}$$

$$I_p = 2 \times I_p / \text{magnet} = 25 \text{ kA},$$

$$I_{\max} = 1.3 I_p = 32.5 \text{ kA},$$

$$di/dt = I_{\max} \times 2 \pi f = 2.917 \text{ kA}/\mu\text{s},$$

We will select the SCR type IR 500PBQ180 or equivalent as discharge switch:

$$I_T (\text{RMS}) = 785 \text{ A}, I_T (\text{AV}) = 500 \text{ A},$$

$$V_{\text{DRM}} = 1800 \text{ V}, di/dt = 400 \text{ A}/\mu\text{s},$$

$$I_{\text{pk}} = 1600 \text{ A (25\% duty cycle, 60 Hz, 400 A}/\mu\text{s}),$$

$$= 3300 \text{ A (according to the conditions used in Fermilab)}.$$

Using the coaxial cable RG 220/U as the transmission line:

$$I_{\text{RMS}} = 100 \text{ A}$$

From the rating values of the SCR above and the coaxial cable, the minimum number of parallel connection of SCR's "n" should be:

$$n = 12 \quad \text{for } I_{\text{RMS}} \text{ of the cable,}$$

$$n = 10 \quad \text{for } I_{\text{pk}} \text{ of the SCR,}$$

$$n = 8 \quad \text{for } di/dt \text{ of the SCR,}$$

It would be desirable to have a higher "n" in order to utilize the best Chinese device, of $di/dt = 200 \text{ A}/\mu\text{s}$, and at the same time to reduce the inductance of the transmission line:

$$\text{select } n = 18$$

$$L_{\text{magnet}} = 1.58 \mu\text{H},$$

$$L_{\text{coaxial cable}} = 12 \text{ m} \times 0.242 \mu\text{H/m}/18 = 0.161 \mu\text{H},$$

$$L_{\text{load}} = 1.58 + 0.161 + 0.215 = 1.956 \mu\text{H},$$

where we assume $L_{\text{stray}} + L_{\text{strip line}} + L_{\text{terminator}} = 0.215 \mu\text{H}$,

$$Z = 1.92L_{\text{load}}/t_r = 0.150 \text{ ohms.}$$

On account of the possible resistance in the load loop and for some tuning range, we add 20% voltage to the minimum required of $(I_{\text{max}}Z)$.

For the Pulse Forming Network (PFN) we have:

$$U_{\text{max}} = 1.2I_{\text{max}} \times Z = 5.85 \text{ kV.}$$

$$\text{Select } C_{\text{PFN}} = 30 \mu\text{F.}$$

for example type MAXWELL 33005 (15 kV, 3375 joules, $0.04 \mu\text{H}$),

$$L_{\text{PFN}} = (Z/0.8)^2 C = 1.055 \mu\text{H}$$

$$\text{Select } L_{\text{PFN max}} = 2L_{\text{load}} = 4 \mu\text{H}, \quad L_{\text{PFN min}} = 0.1 \mu\text{H}$$

$$N_{\text{sections of PFN}} = (t_f + t_r + t_{\text{flattop}})/1.77\sqrt{LC} = 12$$

For M, the number of series connection of SCR:

$$M = 1.5U_{\text{max}}/\text{rating voltage of SCR} = 1.8U_{\text{operation}}/1800 = 4.875,$$

Select $M = 5$

III-4. Calculation of Charge Loop and DC Power Supply

(1) Charge Loop

Waveform: voltage on the PFN capacitor (see Fig IV-3):

For the charging stage, from time t_1 to time t_2 :

$$u = (U_{\text{DO}} - U_0) (1 - e^{-t/\tau}) + U_0, \quad \tau = RC$$

Given:

$$U_{\text{max}} \geq U_{\text{discharge max}} = 5.85 \text{ kV} \quad \text{take } U_{\text{max}} = 6 \text{ kV}$$

$$(t_2 - t_1) < T = 80 \text{ ms,}$$

according to $t_c = 75 \text{ ms,}$

$$\text{take } t_c = t_2 - t_1 = 75 \text{ ms,}$$

$$\text{take } \tau = 30 \text{ ms,}$$

$$C = 30 \mu\text{F/section} \times 12 \text{ sections} = 360 \mu\text{F,}$$

$$U_0 = kU_{\text{max}}, \quad \text{assume } k = (0.7)^2 = 0.5$$

When $t = t_c$, $u = U_{\max}$,

$$e^{-t_c/\tau} = 1 - (U_{\max} - U_0)/(U_{DO} - U_0) = \\ = (U_{DO} - U_{\max})/(U_{DO} - U_R) = \alpha,$$

$$U_{DO} = U_{\max} (1 - \alpha k)/(1 - \alpha) = 6.27 \text{ kV},$$

where $\alpha = e^{-t_c/\tau} = 0.082$, $R = \tau/C = 83 \text{ ohms}$

$$i = I_{\max} e^{-t/\tau} = (U_{DO} - U_0) e^{-t/\tau} R^{-1}$$

$$I_{\max} = 39 \text{ A} \approx 40 \text{ A},$$

$$I_{\text{rms}} = \left(\frac{1}{T} \int_0^{t_c} (I_{\max} e^{-t/\tau})^2 dt \right)^{1/2} = 17.26 \text{ A},$$

$$I_{\text{average}} = I_d = I_{\max} F \tau (1 - e^{-t_c/\tau}) = 13.77 \text{ A},$$

$$P_{DO} = U_{DO} I_{\text{average}} = 86.34 \text{ kW},$$

$$P_R = I_{\text{RMS}}^2 R = 24.73 \text{ kW},$$

energy stored in capacitor (average):

$$(P_{DO} - P_R) T = 4928 \text{ joules}, 411 \text{ joules/capacitor}.$$

(2) Rectifier

Rectifier - 3 phase bridge type:

$$\text{Average current } I_F = I_d/3 = 4.59 \text{ A},$$

$$\text{Max current } I_{FM} = I_F/0.318 = 14.43 \text{ A},$$

$$\text{RMS current } I_{\text{RMS}} = 0.579 I_d = 7.97 \text{ A},$$

$$\text{Reverse voltage } V_{RM} = 1.41 E_L = 1.41 U_{DO} 1.35^{-1} = 6.55 \text{ kV},$$

$$\text{Surge current } I_s = 140 \text{ A (due to } I_{\max} \text{ of commutate loop),}$$

(see below).

We can select Westinghouse Electric Co. compensated high voltage silicon rectifier stacks or International Rectifier Co. three phase full wave rectifier assemblies.

For example: W.H. SE5A09Z0323

I_{DC} OUT	surge current	voltage/cell	cell/module	module/leg
12 A	240 A 1 Hz	1.0 kV	4	3

total number of modules per stack channel = 3 x 6 = 18.

(3) Transformer:

$\Delta || Y$ type

$$E_{line.sec} = U_{DO}/1.35 = 4.65 \text{ kV.}$$

$$E_{\phi.sec} = E_{line.sec}/\sqrt{3} = 2.685 \text{ kV}$$

with taps of $\begin{matrix} +10 \\ -20 \end{matrix} \% E_{\phi.sec}$

$$K = \text{turn-ratio} = 2.685/0.380 = 7/1.$$

$$I_{\phi.sec} = 0.816 I_d = 11.24 \text{ A, take 14 A}$$

$$I_{\phi.pri} = 11.24 \times 7 = 78.68 \text{ A, take 98 A}$$

$$P_{transformer} = 3 \times 98 \times 380 = 112 \text{ kVA.}$$

(4) Charging SCR:

Assume the capacitor bank will be reverse-charged to about 80% of it's original charged value.

The peak off-state voltage which the charging SCR should be capable to stand is:

$$V_{peak \text{ off-state max}} = 6.27 \text{ kV} + 6 \times 0.8 \text{ kV} = 11.07 \text{ kV}$$

With 100% safety margin,

$$U_{design, peak \text{ off-state max}} = 22 \text{ kV.}$$

In order to get a wider range of charging voltage, a SCR with shorter $t_{turn-off}$ should be used, but for such device the rating U_{DRM} will be lower.

We select W.H. T627122064 DN as charging switch:

U_{DRM} U_{RRM}	$I_{\text{T(AV)}}$	$T_{\text{turn-off}}$	I_{GT}
1200 V	200A	20 μ s	150 mA

Number of series connection of SCR
 $n_{\text{series}} = 18.$

(5) Commutating SCR:

(A) Selection of SCR and approximate analysis.

Select T627 121564DN as commutating SCR, it's specification are as follows:

U_{DRM} U_{RRM}	$I_{\text{t(AV)}}$	$T_{\text{turn-off}}$
1200 V	150A	20 μ s

The equivalent circuit of the power supply during the commutating process is as shown in Fig IV-4.

If we neglect R' and i' within short duration (about 20 μ s),

$$i = (U_{d0} \sin w_d t) / w_d L,$$

$$u_c = U_{d0} (1 - \cos w_d t)$$

L : leakage inductance of transformer, according to the one used in Fermilab, $L = 8.5$ mH.

C_{com} : assume to be 4 μ F.

$$w_d = \sqrt{1/LC_{\text{com}}} = 5.423 \times 10^3, \quad T_d = 1.158 \text{ ms},$$

$$I_m \approx U_{d0} / w_d L = 136 \text{ A},$$

$$U_{\text{com}} = 2U_{d0} = 12.54 \text{ kV}$$

(B) The approximate waveforms of these voltages and currents during the charging and commutating process are shown in Fig. IV-5.

During the commutating period, when $E \geq U_{\max}$, the charging SCR will be reapplied by forward voltage, so the condition of maintaining the charging SCR in the off-state is:

$$\Delta t_{E \leq U_{\max}} > \text{rating } t_{\text{turn-off of SCR charge.}}$$

Solve the equation of u_c :

$$u_c = E = U_{d0} (1 - \cos \omega_d t) = U_{\max},$$

$$\Delta t_{E \leq U_{\max}} = 282 \mu s > \text{rating } t_{\text{turn-off}} = 20 \mu s.$$

(C) Number of series connection of commutating SCR's.
For our circuit:

$$U_{\text{DRM}} = 2 \times 6.27 \text{ kV} = 12.54 \text{ kV} \text{ with safety margin 2.}$$

$$\text{RRM}$$

$$I_{\text{max}} = 2 \times 136 \text{ A} = 272 \text{ A} \quad \text{with safety margin 2.}$$

$$I_{\text{av}} = 2I_{\text{max}} (T_d/2) / \pi T = 1.253 \text{ A}$$

So $n = 10$

IV-5. Calculation of Recovery Circuit

The simplified equivalent circuit and waveforms are shown in Fig. IV-6.

Requirements of this circuit:

(1) Efficiency = 0.8--0.9,

(2) Moderate inductance L , so that it will not seriously affect the work of the discharging loop during the fall stage, on the other hand, it will still give enough time for charging the capacitor bank from the reversed charged voltage.

$$u = -U_m e^{-dt} \cos wt, \quad U_m = 0.8 \times 6 \text{ kV} = 4.8 \text{ kV},$$

$$i = I_m e^{-dt} \sin wt,$$

$$d = R/2L, \quad dt_{(\text{recovery})} = R \sqrt{LC}/2L = \pi/2Q.$$

If we use Westinghouse R920 181600 as a free-wheeling diode,

$$U_{RRM} = 1800 \text{ V}, \quad I_{AV} = 1600 \text{ A}, \quad I_{\text{surge}} = 21500 \text{ A},$$

I_{pk} can be (9-10) kA. Assume $I_{pk} = 9 \text{ kA} = I_m$, therefore

$$Z \approx U_m e^{-dt_r/2} / I_{pk} = U_m \sqrt{\beta} / I_{pk} = 506 \text{ m}\Omega, \quad \beta = 0.9,$$

$$L = Z^2 C = 92 \mu\text{H},$$

$$f = 1 / 2\pi \sqrt{LC} = 873 \text{ Hz},$$

$$t_r = T/2 = 572 \mu\text{s},$$

$$Q = \pi / 2dt_r = 15$$

$$R_{\text{allowable}} \leq Z/Q = 34 \text{ m ohms},$$

$$I_{\text{rms}} = \sqrt{t_r/2T} I_p = 538 \text{ A},$$

$$P = I_{\text{rms}}^2 R = 9.85 \text{ kW}, \quad \text{take } P = 10 \text{ kW}.$$

$$I_{\text{av}} = 2t_r I_p / \pi T = 41 \text{ A},$$

$$n = \text{number of series connection of diodes} = 2U_m/1800 = 6.$$

The results of the calculation for the recovery reactor is listed in Table IV-2.

IV-6. Calculation of Current Quenching Circuit

The equivalent circuit is shown in Fig. IV-7.

Suppose the material of the saturable reactor is Deltamax (50% Ni, 50% Fe) with dimensions as follows:

outer diameter = 25 cm
inner diameter = 10 cm,
width of strip = 5 cm,
length of core = 6 x 5 = 30 cm.

Operating induction = 10,000 gauss, which is lower than the saturation induction (16,000 gauss).

The voltage applied across the saturable reactor will approximately be the reverse voltage at the capacitor bank during the period of turning the discharge SCR off. Therefore the time within which the discharge SCR should be turned off can be calculated as:

$$\begin{aligned}\phi_m &= \int_0^{t_{\text{turn-off}}} U_{\text{reverse}} dt = U_{\text{reverse}} \times t_{\text{turn-off}} = 4.8 \times 10^3 t_{\text{turn-off}} \\ &= B_m \times \text{Area} = 4.5 \times 10^{-2} \text{ web,} \\ t_{\text{turn-off}} &\cong 10 \mu\text{s,}\end{aligned}$$

average length of magnetic loop = $\pi(OD + ID)/2 = 55$ cm,
magnetizing force $H = 1$ oersted, (estimated from the curves for 2400 Hz and $1 \mu\text{s}$), so the current through the magnet during this time will approximately be

$$I = 1 \times 55/1.257 = 44 \text{ A.}$$

Further calculation can be done only after measuring the charge Q_{rr} of the discharge SCR. For an estimate suppose $Q_{rr}/\text{SCR} = 400 \mu\text{coulombs/SCR}$, so $Q_{rr} = 400 \times 18 = 7200 \mu\text{coulombs}$. For the circuit shown in Fig. IV-7, we have

$$i = \frac{U}{R} e^{-t/\tau}$$

$$Q_{rr} = \int_0^{t_{\text{turn-off}}} i_{dt} = U \tau (1 - e^{-t_{\text{turn-off}}/\tau}) / R =$$

$$= CU (1 - e^{-t_{\text{turn-off}}/\tau}),$$

$$\tau = t_{\text{turn-off}} / \ln [C.U / (C.U - Q_{rr})], \quad C = 360 \mu F,$$

$$\tau = 2394 \mu s,$$

therefore:

$$R = 6.65 \text{ ohms},$$

$$I_{\text{max}} = 4.8 \text{ kV} / 6.65 \text{ ohm} = 720 \text{ A}.$$

So we should at least take parallel connections of 2 SCR's with rating $di/dt > 400 \text{ A/s}$, each branch should be 5 SCR's in series connection, as shown in Fig. IV-8.

IV-7. Firing Circuit and Protection of SCR's

All of the SCR switches are triggered and isolated from each other by using gate amplifiers and transformers.

For synchronization of the operation of the SCR's in the same switch, the primary windings of the isolating transformers are connected in series.

For increasing the rising slope of the trigger voltage and turning off the SCR of the gate amplifier after the duration of its conduction we can utilize a resonant circuit consisting of the inductor of the primary winding of the isolating transformer and the capacitor across the DC power supply.

In principle, the trigger circuit is the same as used in Fermilab, the only difference being the use of one transformer for each parallel branch rather than two parallel branches. Eighteen transformers will be required for exciting the discharge switch, the cores and the voltage of the power supply of the gate amplifier will be then larger.

For the protection of the SCR's there are AC and DC "snubber" circuits to be used.

(i) DC Voltage Balance:

The average voltage for each discharge SCR is: $6 \text{ kV}/5 = 1200 \text{ V}$. Suppose the allowable maximum and minimum voltage of unbalance are 1500 V and 900 V respectively. The balancing resistor is $100 \times 10^3 \text{ ohms}$, then the allowable difference of leakage current for the SCR's will be

$$\Delta I = \Delta U/R = (1500-900)/100 \times 10^3 = 6 \text{ mA}$$

If the maximum leakage current is 10 mA , the allowable range of leakage should be $7 \text{ mA} \pm 3 \text{ mA}$.

The power consumption of the resistor will be

$$\begin{aligned} P &= U_{\text{rms}}^2/R = \text{duty cycle} \times U_{\text{max}}^2/R = \\ &= 60 \times 10^{-3} \times 12.5 \times 1500^2/100 \times 10^3 = 17 \text{ W} \end{aligned}$$

With 50% safety margin we choose 25 W .

(ii) AC snubber:

If for a $C=1 \mu\text{f}$ and $\Delta U = 600 \text{ V}$, the allowable difference of recovery charge between two SCR's in series connection will be:

$$\Delta Q = C \Delta U = 1 \times 10^{-6} \times 600 = 0.6 \times 10^{-3} \text{ Coulombs.}$$

For limiting the di/dt of the SCR's from the capacitor discharge in the snubber circuit the larger value of R which is in series connection with C is desirable, but di/dt of the SCR's when turning off will be larger; as a compromise we select $R=15 \text{ ohms}$.

iii) Current Balance in Parallel Branches:

We connect the discharge SCR in series first, then connect these chains in parallel, it averages the forward characteristics of SCR's in the series chain, improving the balance of the currents in the parallel branches.

For further improving the current balance in the parallel branches we utilize the inductance of the transmission cable as a balancing reactor.

$$L = 0.24 \mu\text{H/m} \times 12 = 2.88 \mu\text{H}.$$

The Fermilab experience is that this is enough for this purpose. The circuit diagram for firing SCR's is shown in Fig. IV-9.

IV-8. Voltage Regulator and B Coil

(i) Voltage Regulator:

Assume the voltage ratio of the voltage divider is 750:1 and set the voltage from the standard Zener diode is 6.3 V (Fig. IV-10).

According to the calculated charge voltage we set the minimum regulator voltage being:

$$6.3 \text{ v} \times (R_{f1}/R_1) \times \text{voltage ratio} = 1500 \text{ V},$$

and the maximum regulator voltage being:

$$6.3 \text{ v} \times R_{f1}/R_1 + (R_{f1}/R_2) \times R_4/(R_3+R_4) \times \text{voltage ratio} = 5862 \text{ V}.$$

The value of the overvoltage protection is:

$$6.3 \text{ V} \times (R_{f2}/R_5 + R_{f2}R_4/R_6 (R_3 + R_4)) = 6000 \text{ V}.$$

(ii) $\overset{\circ}{B}$ Coil for the Magnet Current Measurement:

The output of the $\overset{\circ}{B}$ coil integrator is (Fig. IV-11):

$$e_0 = (1/\tau) \int \psi dt = (1/\tau) \int (AN\mu_0/h) (di/dt) dt$$

N: number of turns = 1,

A: area of $\overset{\circ}{B}$ coil in m^2 ,

$$\mu_0: 4 \times 10^{-7},$$

I: magnet current in amps = 32.5 kA,

h: magnet gap in m = 0.056 m,

τ : time constant of the integrator = 6.6×10^{-5} sec,

suppose $e_0 \max = 8$ V, ratio $I/e_0 = 5$ kA/V,

$$A = e_0 \tau h / N \mu_0 I = 5.882 \times 10^{-4} m^2.$$

If the coil length is 5 cm, then the coil width should be:

$$W = 1.176 \text{ cm}$$

IV-9 Interlocks (General Description)

There are eight protections in the interlock system, namely: overvoltage, overcurrent, water flow, vacuum pressure, magnet, safety system, ground fault, and power supply enclosure doors.

Each type of protection has both local and remote indication.

The whole interlock is provided with a separate 3 kVA control transformer, followed by a 24 V DC rectifier.

Every time the supply is turned on (or off) the interlock system will cause the H.V. crowbar to switch-off (-on) and the main contactor to switch-on (-off). Any fault makes the H.V. crowbar to switch-on and the main contactor to switch-off.

With the power supply control in the local mode, the remote control is disabled.

Overvoltage protection is realized through setting the threshold of the overvoltage detection on the voltage regulator board.

Overcurrent is detected by a shunt in the path of H.V. rectifier, which excites a switch-type meter, utilized both for current indicator and protection switch.

Each water branch has a switch and indicator, mounted on the rear rack. All these switches are in series, and there is a general indicator on the front panel. Any failure in one branch of the water system will cause its own and general indicators to turn off.

IV-10.Acknowledgement

It is a pleasure to acknowledge the support of Ken Bourkland, the designer of the original "Orbump" power supply at Fermilab, this project is completed under his assistance. We acknowledge the help and guidance of Carlos Hojvat who gave us many valuable suggestions. The help in the design of the recovery reactor from Stan Snowdon is acknowledged.

IV-11. References

1. Ken Bourkland, "A 35 kA Rapid Cycling PFN Power Supply for Driving Injection Magnets", IEEE Trans. Vol. NS-36, No. 3, June 1979.
2. Carlos Hojvat, "The Multiturn Charge Exchange Injection System for the Fermilab Accelerator", IEEE Trans. Vol. NS-36, No. 3, June 1979.
3. Ken Bourkland, technical notes.

TABLE IV-1

DATA TABLE OF THE ORBUMP POWER SUPPLY

Load inductance L_{load}	1.58 μ H/magnet
Quantity of magnets	4
Peak current $I_{pk}/magnet$	12.5 kA
I_{max}	32.5 kA
Duration of flat top of pulse	60 μ s
Fall time of pulse	30 μ s
Repetition rate	12.5 pps
di/dt_{max}	2.917 kA/ μ s
Impedance of PFN	0.150 ohms
U_{max}	5.85 kV
Sections of PFN	12
C/section of PFN	30 F
L/section of PFN	max 4 μ H min 0.1
Number of discharge SCR	18 p 5s
Number of charge SCR	18 s
Number of commutate SCR	10 s
Number of by-pass SCR	2 p 5s
HV of DC power supply	6.27 kV

TABLE IV-2

DATA TABLE OF THE RECOVERY REACTOR

Mechanical:

Gap	8 cm
Pole width	20 cm
Lamination thickness	0.018 cm
Stacking factor	0.9
Magnet length (18x10.2)	183 cm
Magnet width	50.8 cm
Iron weight	1082 kg
Conductor cross section	1 cm by 2 cm
Number of turns	4
Conductor weight	27 kg

Electrical:

Inductance at 1000 Hz	95 μ H
Quality factor at 1000 Hz (eddy currents only)	60
Practical quality factor approximately	15
Peak magnetic field in iron	6.5 kgauss
Peak current	9 kA
Peak voltage	4.7 kV
Pulse shape: half sinewave, frequency	875 Hz
Repetition rate	12.5 Hz
Average power	4-6 kW

Thermal:

Number of cooling paths	1
Pressure drop	6 kg/cm ²
Cooling water flow	6.8 /min
Temperature rise	4° C
Cooling water hole diameter of conductor	0.32 cm

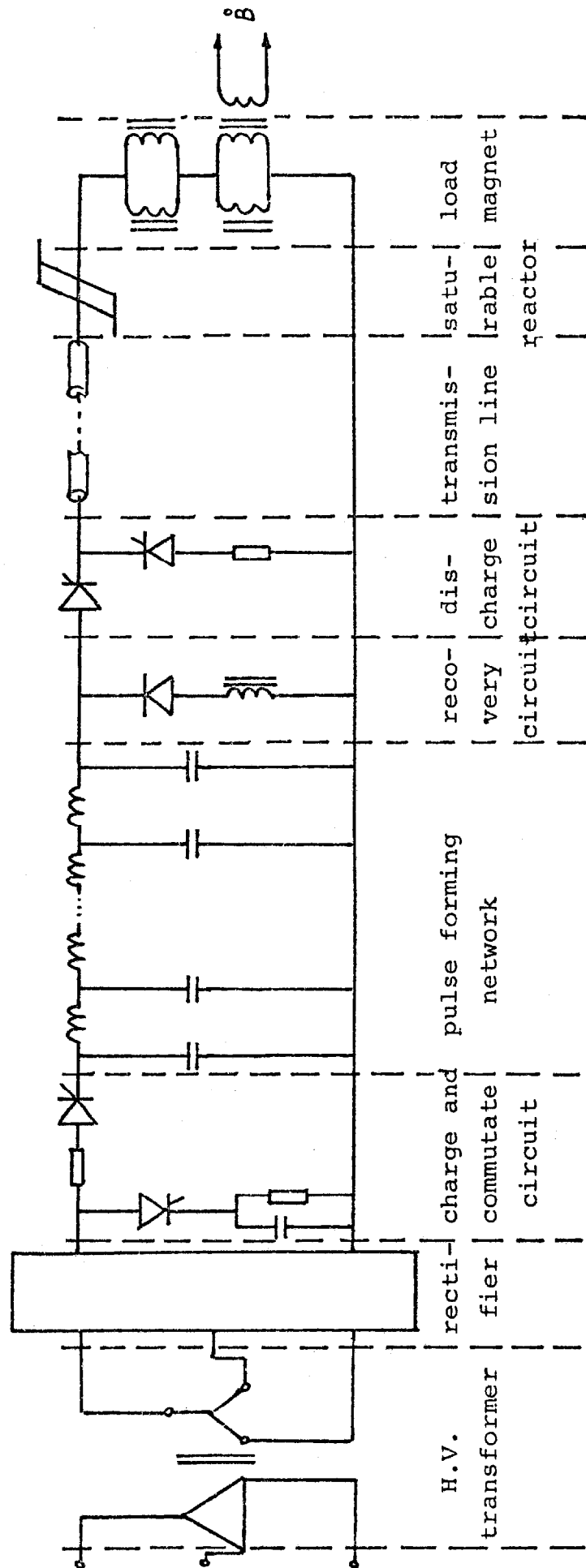


Fig.IV-1. Functional Schematic Diagram.

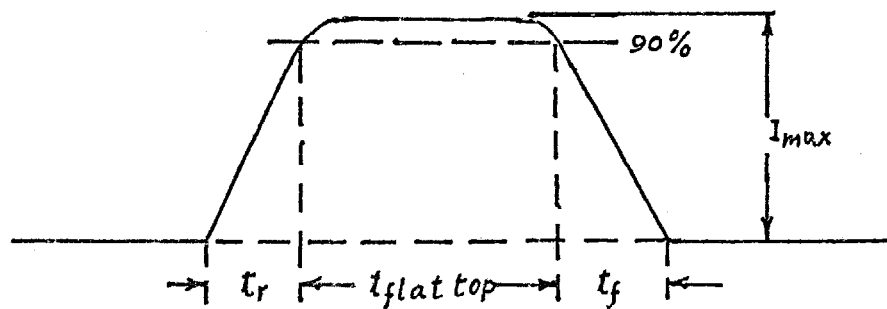


Fig.IV-2. Current Pulse Waveform.

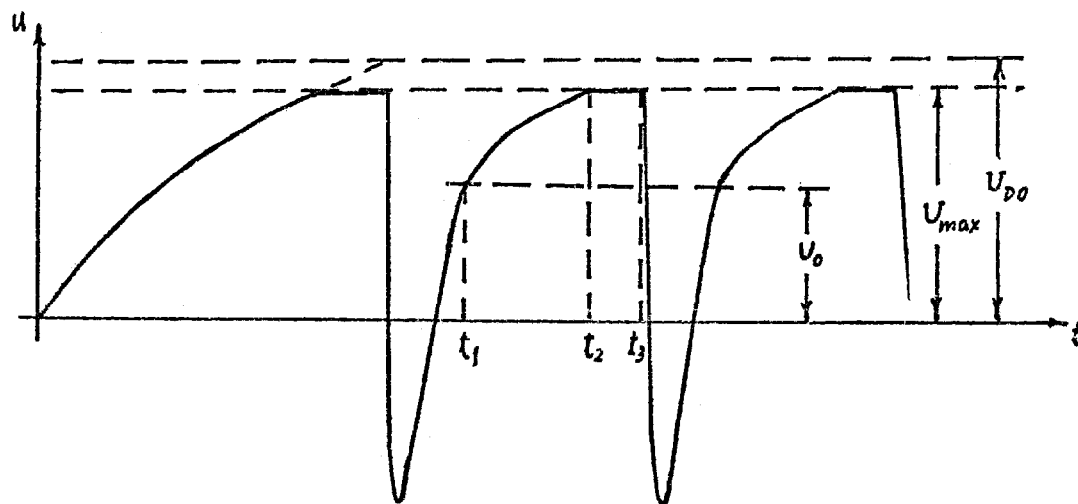


Fig.IV-3. Voltage Waveform On the PFN Capacitor.

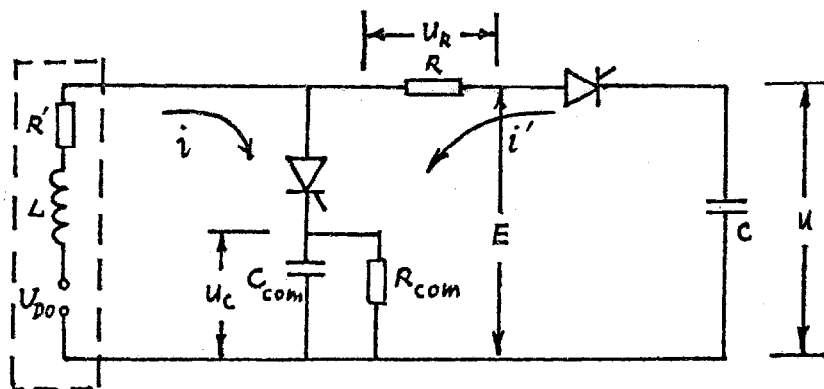


Fig.IV-4. Equivalent Circuit during the Commutating Process.

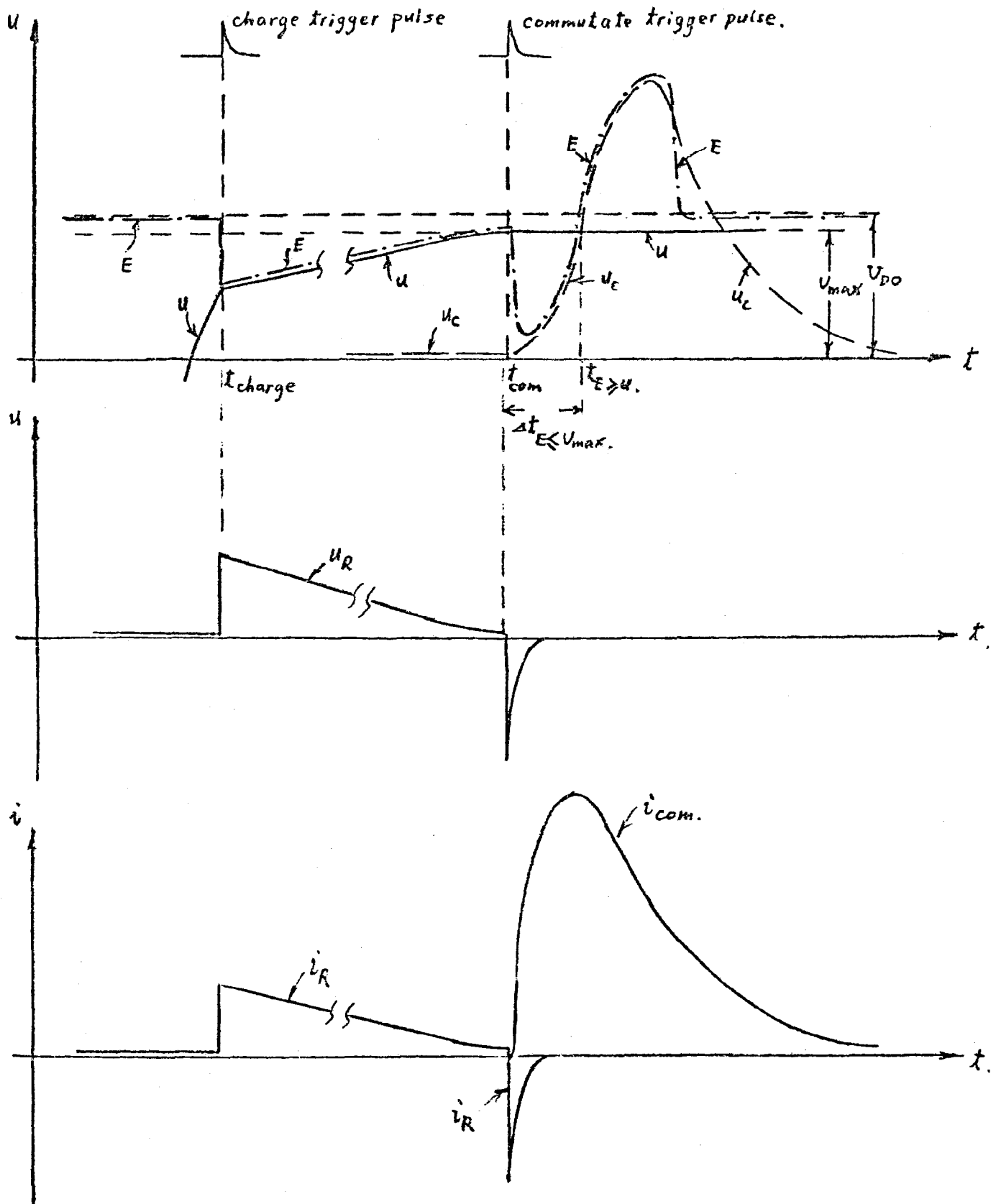


Fig.IV-5. Voltage and Current Waveforms during the Charging and Commutating Process.

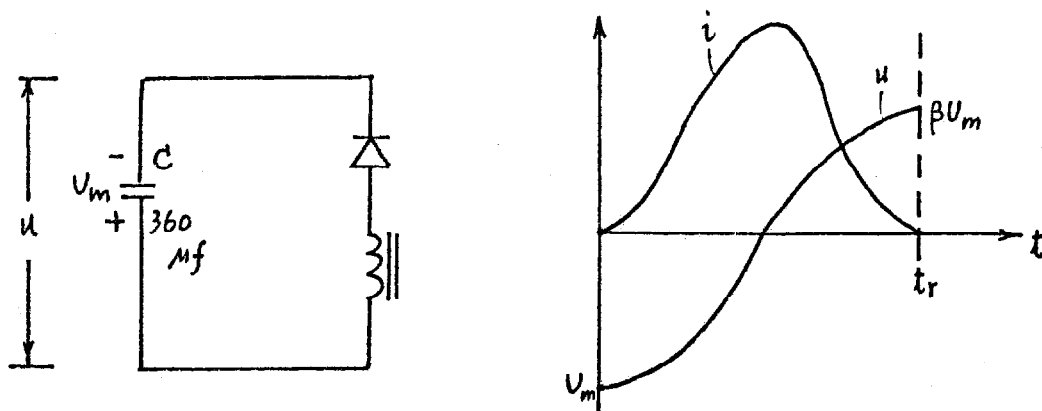


Fig. IV-6. Simplified Recovery Circuit and its Waveforms.

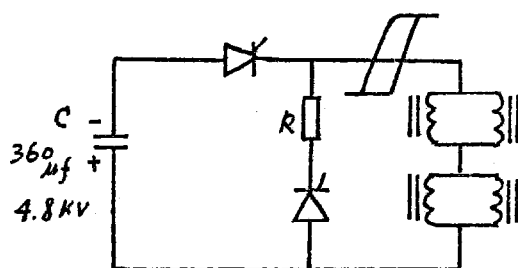


Fig. IV-7. Current Quenching Circuit.

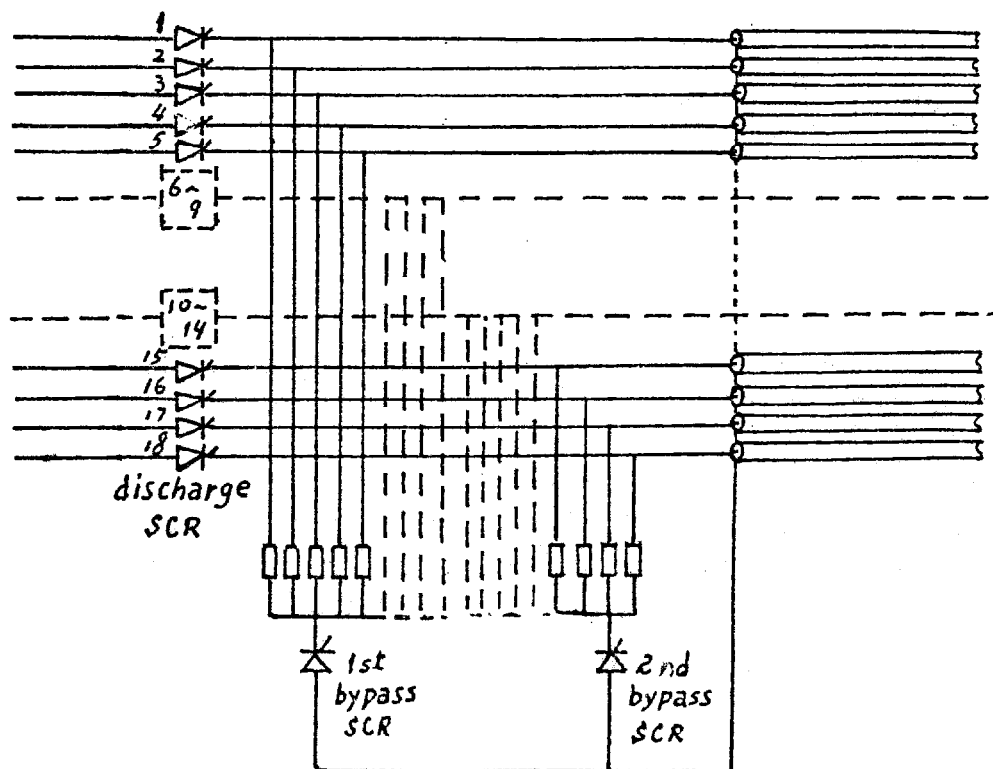
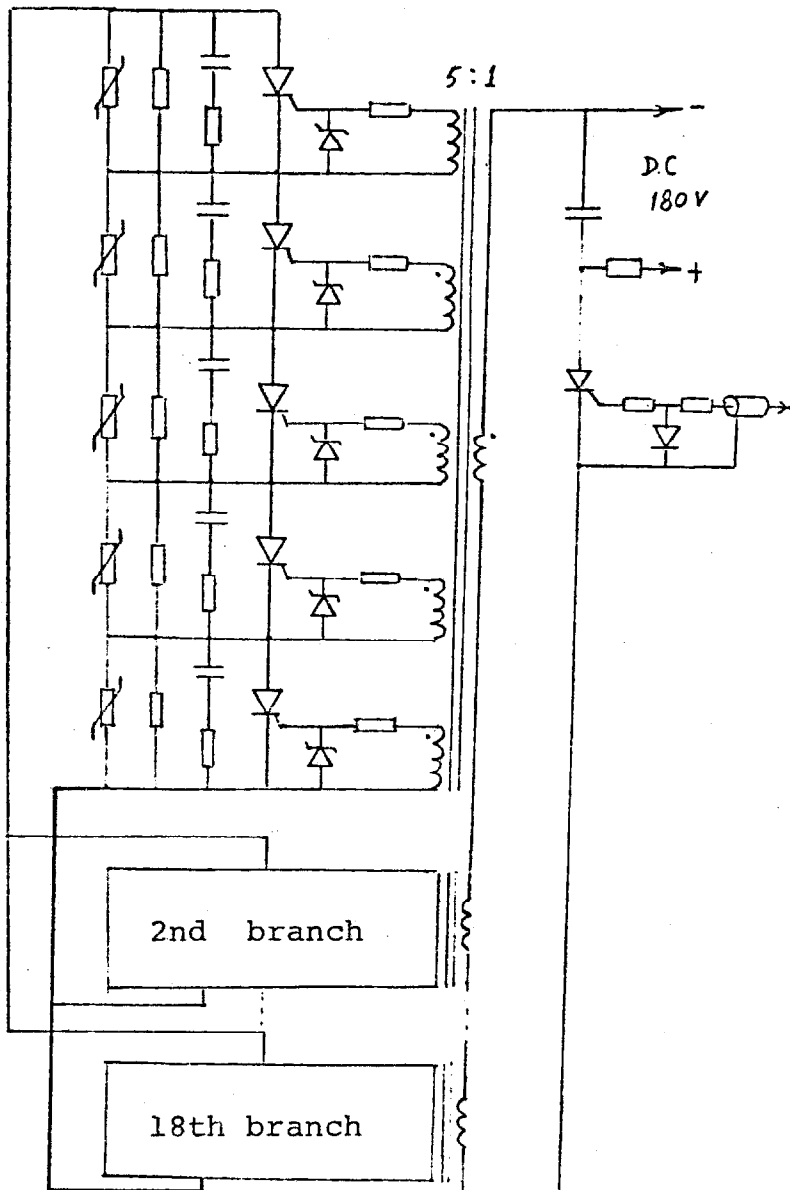


Fig. IV-8. Connection of the Bypass SCR's with the Discharge SCR's.

Discharge trigger circuit

1st branch



Charge trigger circuit

1st group

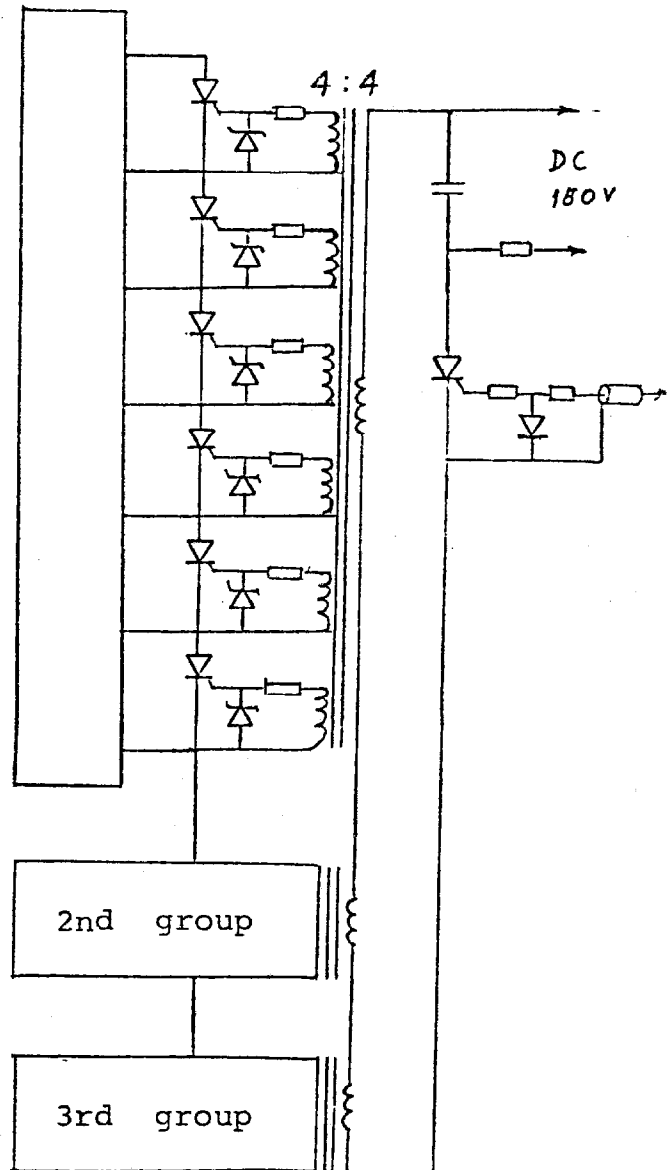


Fig IV-9

Commutate trigger circuit

5 SCR per each group

number of transformer: 2.

turn ratio: 6:4 .

By-pass trigger circuit

5 SCR per each branch

number of transformer: 2.

turn ratio: 6:4 .

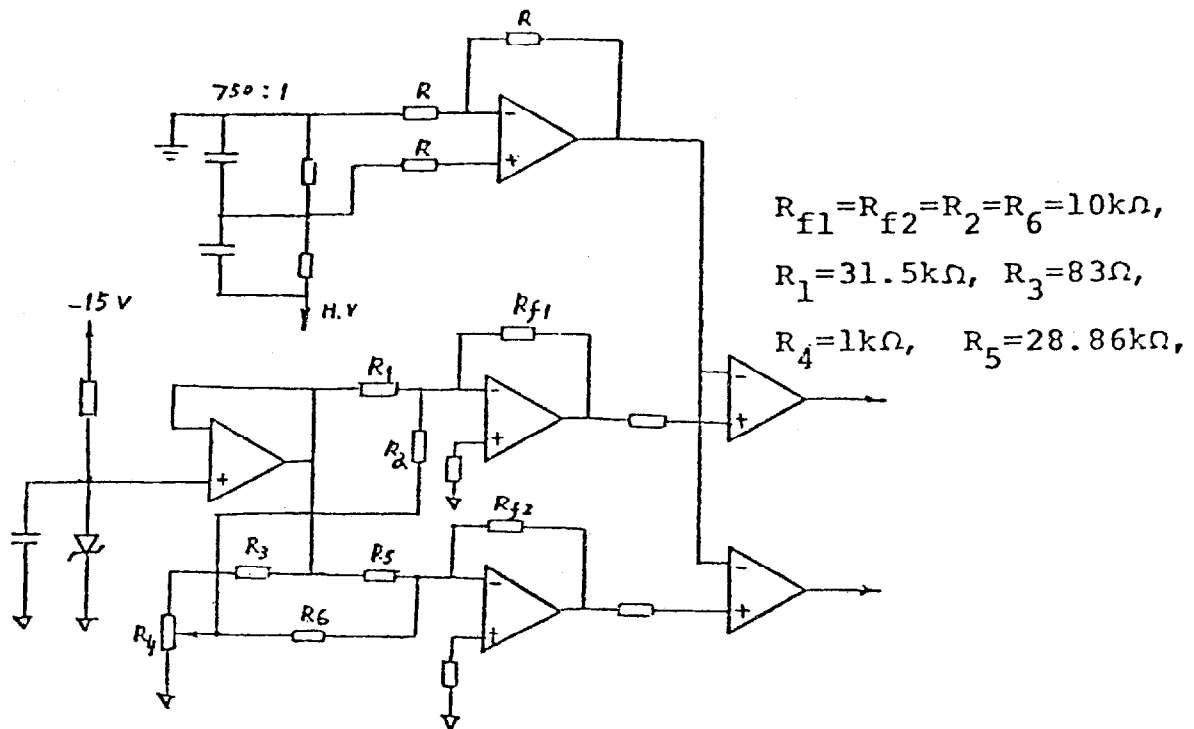


Fig.IV-10. Simplified Voltage Regulator Circuit.

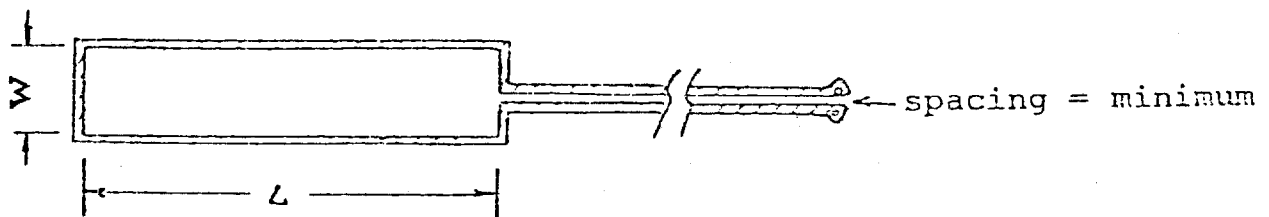


Fig.IV-11. The \vec{B} Coil.

DIAGNOSTICS FOR THE BEIJING BOOSTER INJECTION SYSTEM

Xiao Yi-Xuan

V-1 Description of the Diagnostic Equipment

The diagnostic equipment is proposed to consist of 4 sets of horizontal and vertical single wire scanners (SWH_i, SWV_i), one set of horizontal and vertical multiwire scanners (MWH, MWV), and three beam current transformers (TOR). The H^- dump (H^-C) and the electron catcher (eC) are electrodes to monitor the fractions of unstripped H^- ions and stripped electrons respectively. The H^0 Dump (H^0C) is an electrode to monitor the number of neutral H^0 particles. The H^- and H^0 Dumps are not only used to monitor the beam charged fractions, but serve also to stop the ions in order not to produce residual radioactivity in other accelerator components. The H^+ obstacle (H^+C) is an interim electrode to stop and monitor the proton beam during tuning of the injection system.

The stop H^-S protects the foil changer and the toroid TOR1 in case of failure of the ORBMP power supply. The location of the diagnostic equipment is shown in Fig. I-2.

V-2 Electron Catcher

The kinematic energy of the incident H^- ions is 93 MeV. The maximum energy of the stripped electrons is $93 \text{ MeV}/1836 = 51 \text{ KeV}$. Its magnetic rigidity is $B\rho = 770 \text{ gauss-cm}$ and its maximum velocity $v = 0.4c$. The energy loss for electrons in the Carbon foils can be calculated according to reference (1) by extrapolating to lower energies. The energy loss of electrons is about

$$\frac{1}{\rho} \frac{dE}{dx} = 10 \text{ MeV cm}^2/\text{g}.$$

For $70 \mu\text{g/cm}^2$ thick Carbon foils $E = 700 \text{ eV}$ and $\frac{E}{E_0} = \frac{700 \text{ eV}}{51 \text{ KeV}} = 1.37\%$. Thus a large fraction of these electrons will not stay in the foil. As they move forward they encounter the fringe

field of the bump magnet MHI-3. Due to their low momentum they are bent by the fringe field, travelling back towards the foil. A cylindrical electrode with positive voltage around the foil will be used to collect the electrons either directly from the foil or those bent back by the fringe field. The eC aperture should be large enough to accept the circulating beam. The cylindrical electrode will be made of Aluminum with a diameter of 15 cm. See Figure V-1.

A variable power supply applies to the eC a positive voltage and a signal cable is used to measure the current and relay it to the control room. The signal pulse width will be about $60 \mu\text{s}$ long, with a repetition rate of 12.5 ps^{-1} . According to the calculated conversion efficiency⁽²⁾ H^- (93 MeV) H^+ (93 MeV) for a Carbon foil thickness of $70 \mu\text{g}/\text{cm}^2$ approaches 99%. The H^- ions intensity is 30 mA. Two electrons are stripped from each one of the H^- ions, so the stripped electrons intensity is 60 mA. At the same time that stripping takes place, the H^+ and the electrons bombarding the foil yield secondary electron emission. The secondary electron emission coefficient is a function of the incident particle energy and surface condition of the material. For H^+ the theoretical formula of secondary electron emission γ_{H^+} is⁽³⁾

$$\gamma_{\text{H}^+} \propto \frac{M}{mT} \ln \left(\frac{mT}{M} \right)$$

M, m are the masses of H^+ and e respectively, and T the kinetic energy.

In reference (3) for Aluminum we find the calculated and measured results for which the highest energy is 4 MeV.

Energy (MeV)	0.7	1.0	2.0	3.0	4.0
γ_{H^+} for Al(cal.)	1.43	1.08	0.59	0.41	0.32
(meas.)	1.31	1.08	0.68	-	-

We use these results for Carbon foils and extend them to

93 MeV according to the relation $\mu_H + \alpha \frac{1}{T} - \ln T$. For 93 MeV we estimate the μ_H about 0.05. Then the intensity is 30 mA x 0.05 = 1.5 mA.

Secondary electrons are also emitted by materials when bombarded by electrons. The number of secondary electrons is dependent on the primary electron energy and the angle of incidence of the primary electrons with respect to the surface, as well as on the properties of the material being bombarded⁽³⁾. When the primary electron energy is 300 eV the secondary electron emission coefficient μ_e reaches 1 for Carbon (graphite) and Aluminum. Above and below this energy $\mu_e < 1$. For a primary electron energy of 51 KeV the $\mu_e < 0.1$. Most secondary electrons are emitted with low energy, with the most probable energy in the range of 1-10 eV. The contribution from this effect could be as high as 60 mA x 0.1 = 6 mA. The electron catcher collects all the stripped electrons from H^- ions and all the secondary electrons. The total electron intensity collected by the catcher is 60 + 1.5 + 6 = 67.5 mA maximum. For an applied voltage on the catcher of 200 V, the maximum power is: 200 V x 67.5 mA = 13.5 watts per pulse.

The injection pulse is 60 μ s long and the duty cycle is 12.5 c/s, thus the average power is very small (= 10 mW). The collected electron current circulates through a resistor on the ground side of the supply. This voltage signal is sent to the control room by a signal cable.

In order to separate the injected turns we have to measure the stripped electron intensity for one turn (1.1 μ s) of injection, and we require a pulse time resolution of 0.1 μ s. See Figure V-1.

V-3 H^- Dump and H^- S Stop

In the case of foil failure the H^- ions will be unstripped, bending in the reverse direction of that for the protons. The H^- dump H^-C is used to stop them, before they strike the vacuum chamber, in front of the bump magnet MBHI-4. H^-S stops the H^- beam in case of the ORBMP power supply failure during injection.

The range for 93 MeV protons is 3.3 cm in Aluminum and 1.2 cm in Copper.

The intensity of the H^- beam is of the order of 30 mA per pulse. The pulse length is $60 \mu s$, and the repetition rate is 12.5 c/s. Then the average power loss on the H^- Dump is:

$$93.10^6 \text{ eV} \times 30 \cdot 10^{-3} \text{ A} \times 60 \cdot 10^{-6} \text{ s} \times 12.5 \text{ c/s} = 2.1 \text{ kW}$$

At the position of the H^- Dump the cross-section of the injected H^- beam is $2.7 \times 1.1 \text{ cm}^2$. We take the area of the dump as $6 \times 6 \text{ cm}^2$, 4 cm thick for Aluminum and 2 cm thick for Copper. The temperature rise of the H^- Dump will be:

Material	Weight	Heat Capacity (293°K)	Rise in Temperature
Aluminum	388.8 gm	5.81 cal/gmole	6.0 °C/S
Copper	645.1 gm	5.85 cal/gmole	8.5 °C/S

The water flow required to removed 2100 Watts for a rise of the water temperature of 30°C is:

$$Q = \frac{2100}{4.2 \times 30} = 16.7 \text{ l/s} = 251 \text{ gpm}$$

this amount of water flow is too large to be incorporated into the dump design. With the accelerator operating at full injected current, the dump should be interlocked such that the H^- beam is shut off within one minute of impinging on the dump. The beam current on the dump can be monitored as shown in Figure V-2.

If we assume that a water flow of 0.007 l/s (0.1 gpm) can be achieved then the average beam power must be reduced to the order of 1.0 watts. This can be achieved by reducing the repetition rate, the beam intensity and the length of the beam pulse.

V-4 H⁻ Dump

For the 93 MeV H⁻ ion traversing the 70 $\mu\text{g}/\text{cm}^2$ Carbon foil the H⁻ \rightarrow H⁰ conversion efficiency is of the order of 1%. The H⁰ particles continue straight through the bump magnets MBHI-3 and MBHI-4 and the first focusing magnet. To prevent the buildup of residual radioactivity they should be stopped before the vacuum chamber and the magnet coils. In order to have enough separation between the H⁰ beam and the circulating protons the best position is to set the H⁰ stop downstream of the first F-magnet.

The thickness of the stop metal plate will be the same as for the H⁻ Dump. Although the intensity is 1% of the H⁻ ions intensity. For simplicity we will utilize the same design of the H⁻ Dump for the H⁰ Dump. The limitation on the average beam power allowed on the Dump should be remembered.

The scheme for the H⁰ Dump is also shown in Fig. V-2.

V-5 H⁺ Obstacle

When we start to tune the injection system we would like to measure the beam position and intensity of the injected beam with no circulating beam. The H⁺ obstacle could be set remotely in front of MBHI-2 to stop the circulating beam before starting the second turn. The design of H⁺ obstacle is the same as the H⁻ Dump. The same limitation on average beam power applies here.

V-6 Beam Current Transformer (TOR)

The injected beam intensity will be nondestructively measured by means of beam current transforms at 3 points. They are situated at the injection point, the upstream and the downstream ends of the injection straight. The proton beam passing through a toroidal core induces a voltage in a 100 turn sense winding. The wound core of the transformer will be made of thin permalloy film (0.05 mm thickness) whose permeability is about 3×10^4 . The dimensions of the core are 17 cm o.d. x 15 cm i.d. x 2 cm height. The system is sensitive enough to measure the beam over one revolution or in the injection line.

The required performance of the system is as follows:

Dynamic range 1 mA ($= 10^{11}$ ppp) \rightarrow 100 mA ($= 10^{13}$ ppp)

Frequency response 10 kHz \rightarrow 100 MHz

Rise time 10 ns

Decay time 1 ms

Measurement Accuracy 1% ($= 10$ mA).

The signal should be available and digitized for display in the control room.

V-7 Multiwire and Single Wire Scanners

Beam profiles will be measured using wire secondary emission monitors. One set of horizontal and vertical multiwires will be installed at the upstream and one set of horizontal and vertical single wire at the downstream end of injection septum. Another three sets of single wire scanners will be installed at the following locations: downstream of MBHI-2 (SWH2,SWV2), downstream of MBHI-3 (SWH3,SWV3), and at the starting point of the injection straight section (SWH4,SWV4).

The wire scanners should have a time response fast enough to observe single turn beam pulses. The wire is 0.01 mm diameter tungsten. The position of the wire can be controlled remotely with an accuracy of 0.1 mm from the control room. The range of the current induced in the wire is 1 to 10 mA ($10^8 \rightarrow 10^9$ ppp) with a required measurement accuracy of about 0.1 mA. This is an extremely simple method of making high resolution profile measurements. During the scan, the current on the two wires is read by the computer. Although this technique is slower than others (for example, residual gas ion measurements) it offers the advantage of higher resolution with analog data channels. Signal strengths are large enough to allow the current amplifiers to be located outside the radiation area.

The data obtained with the single wire scanners could be used for determining the beam emittance as three horizontal and vertical profiles will be measured within a straight section.

V-8 T.V. Camera

It has been Fermilab's experience that at least during implementation of the injection system, a T.V. camera to monitor the foil position and integrity is very useful. Furthermore, if during acceleration the beam hits the foil due to radial changes in the orbit this can be observed as the foil could become red hot. This particular location requires not only a radiation resistant T.V. camera but also illumination of the foil.

A radiation resistant camera has lenses that form color centers after large amounts of accumulated radiation and that are also simple to diffuse out. Also the amplifier video section is separated from the camera into a radiation free area.

V-9 Commissioning of the Injection System

The restriction on maximum beam average power allowed on the H^- , H^0 and H^+ Dumps as discussed on V-3, should be remembered in the following discussion

A. Measure the position, size and divergence of the H^- ion beam at the entrance of the septum, in order to tune the 93 MeV H^- ions transport system to assure matching with the Booster lattice.

B. Measure the position of the center of the injected beam at the exit of the septum. During SWH-1 and SWV-1 scans the current on the two wires should be maximum vertically at the center of the aperture and horizontally at 0.11 m outside the booster center orbit.

With the foil removed the H^- ions are collected by the H^- Dump H^-C .

C. SWH-2 and SWV-2 are used to measure the position of the center of the beam at the foil position. By adjusting the current in the bump magnets the beam can be adjusted to the injection position horizontally. Vertically the trim magnets in the injection line are used to set the injected beam horizontally.

D. Putting the stripping foil in the injection point, the signal from the H^- Dump should disappear. The beam of protons should now coincide with the center orbit of the booster at the wire scanners SWH-3 and SWV-3. The H^+C could be used as the H^+ obstacle to prevent the beam from circulating in the Booster until the injection geometry is understood.

E. The H^0 Dump is removed. With the main magnet system properly adjusted the beam will return back to the injection straight section. SWH-4 and SWV-4 can be used to determine that the beam is back to the nominal center orbit. The H^+ obstacle can be used to obstruct the circulating beam to understand the one turn operation.

F. Removing the H^+ obstacle, SWH-2 and SWV-2 can be used to insure that the bumped orbit coincides with the incident beam for multiturn injection.

G. Toroids 1,2,3 monitor the intensity of the proton beam. Toroid 1 and the H^+C monitors the intensity of the H^- beam when the foil is not in place.

H. Lengthen the H^- ions pulse to allow multiturn injection. The H^+ obstacle stops the protons from circulating. According to the method provided in reference (4) we can measure the foil's efficiency for electron stripping. Also the stability of the injection system can be studied over the longest injection times ($60 \mu s$).

V-10 Acknowledgements

The author wishes to acknowledge the help and support of his teacher Dr. C. Hojvat.

References

- 1) W. Galbraith, W.S.C. Williams, High Energy and Nuclear Physics Data Handbook, p VII-15.
- 2) Xiao Yi-Xuan, Internal Report, HEP Institute Academica Sinica (1979).
- 3) S.N. Ghosh, S.P. Khare, Phy. Rev. Vol. 125 No 4, p. 1254 (1961).
- 4) R.C. Webber, C. Hojvat, IEEE NS-26, No. 3, p 4012 (1979).

Foil Electron Catcher

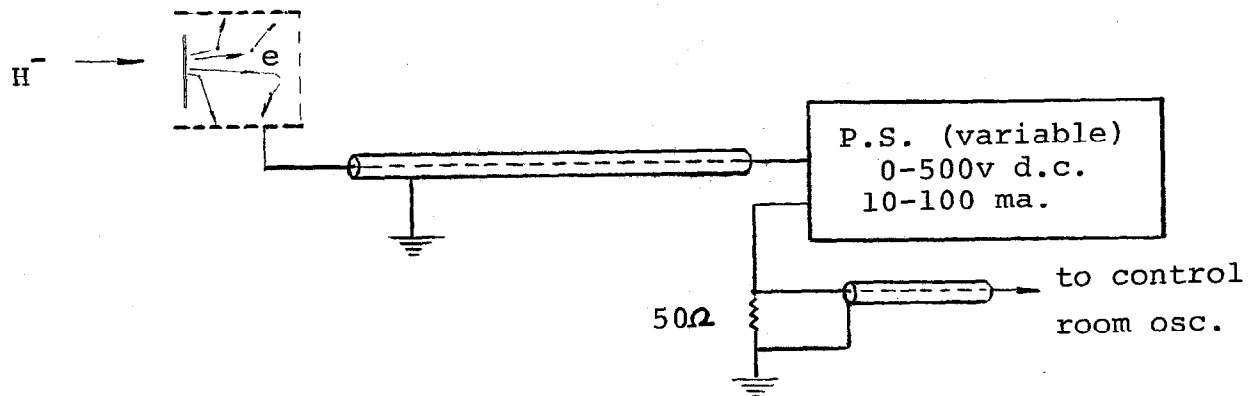


Figure V-1 Electron Catcher

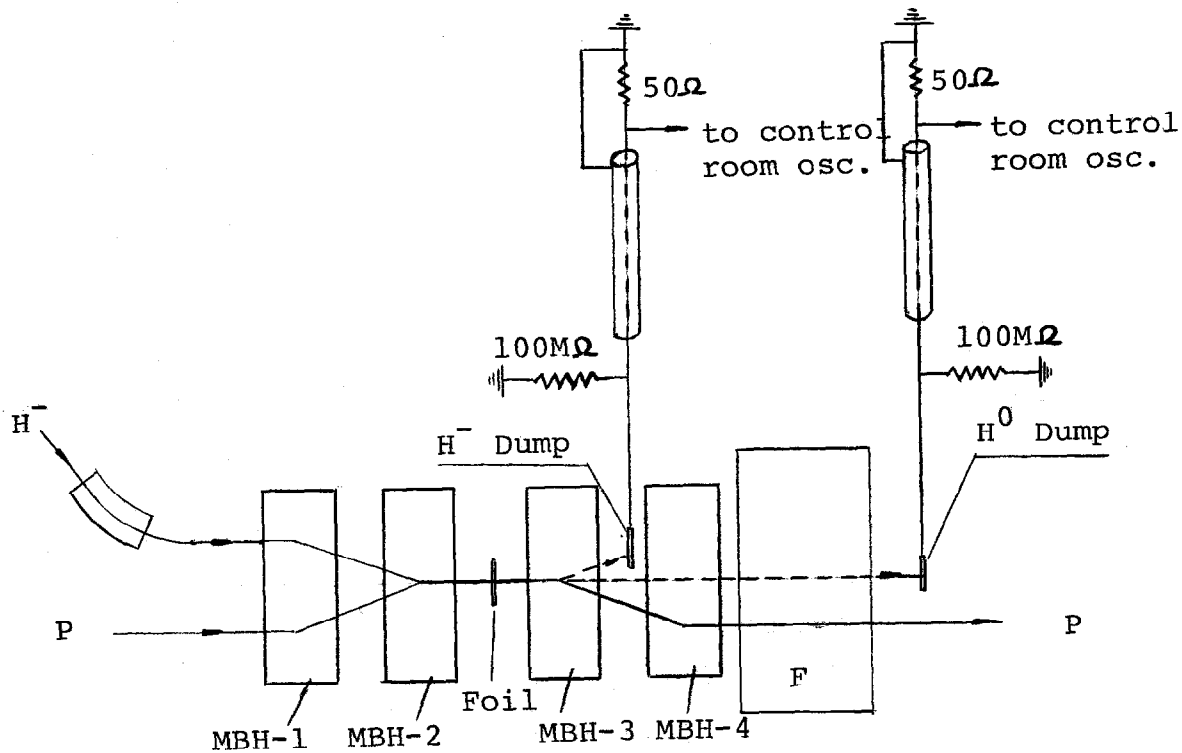


Figure V-2 H^- Dump and H^0 Dump

CHAPTER VI

SUMMARY

The previous chapters present a detailed and comprehensive design for a Charge Exchange Injection system for the Beijing Booster. We have followed closely the Fermilab Booster design as it has proven to be very successful after more than one year of operation.

A project of this kind is only a small and important part of a larger design effort. It is an integral piece of the rest of the facilities at the Beijing Institute of High Energy Physics. As such, this report can be considered final only as far as the rest of the designs are.

Throughout this report emphasis has been put on utilizing components made in the People's Republic of China. It is hoped that the specifications required for many other components could be obtained from Chinese industry. Monetary considerations may require the revision of some parts of this design.

The most delicate part of the Charge Exchange Injection is no doubt the stripping foils. The Carbon foils could be purchased in the U.S.A., although the cost over many years could become prohibitive. Enough effort was put into the manufacturing techniques to enable the Beijing Institute to develop their own facilities. The mounting of foils to the specifications of this report was successfully achieved by the Chinese colleagues using foils of the same source as Fermilab. Considerable mechanical design has gone into the device to store and remotely exchange foils within the Booster. This work is not reported here as it may need to be completed in the PRC.

In order to integrate the present injection into the Beijing Booster a significant mechanical design effort is required to locate the devices in the straight section, to provide for alignment, vacuum, interconnections between magnets and power supplies, remote positioning, and interface with the control computer. Only part of these items have been started and do not form part of this report.

The injection group of the Beijing Booster arrived at Fermilab the end of November 1979. The working schedule was organized by Dr. C. Hojvat and put into execution at the beginning of December. The division by subject, their present status and the personnel involved is as follows:

Item	Description	Status	Work Remaining	Person Responsible	Advisor
1.	Specifications of the booster injection parameters	Completed		C. Zhang	C. Hojvat
2.	Stripping foil Calculations	Completed		Y.X. Xiao	C. Hojvat
3.	Specification of the diagnostic parameters	Completed		Y.X. Xiao	C. Hojvat
4.	Layout of foil handler, and electron catcher	Assembly drawing Completed	Detailed drafting	Y.D. Hao*	D. Cosgrove
5.	Beam detector, H ⁻ dump	Not Started		Y.D. Hao*	D. Cosgrove
6.	Orbump design	Assembly drawing	Detailed drafting	Y.S. Shi	D. Cosgrove
7.	Septum design	Assembly drawing	Detailed drafting	Y.S. Shi	D. Cosgrove

Item	Description	Status	Work Remaining	Person Responsible	Advisor
8.	Pulsed power supply for orbump	Completed		Y.L. Jiang	K. Bourkland
9.	Pulse power supply for septum	Changed to D.C. supply		Y.L. Jiang	K. Bourkland
10.	Detail of the Long straight mechanical design	Not started		Y.S. Shi	D. Cosgrove
11.	Vacuum system	Not started		Y.S. Shi	D. Cosgrove

NOTE: *Work performed by Y.S. Shi.

The work schedule is for the most part finished. The Chinese Group appreciates their advisors for their help and techniques. During this collaboration a great spirit of friendship and understanding has been built. The members of the group also acknowledge the help and advice from L.C. Teng, C.W. Owen, Q.A. Kerns, S.C. Snowdon, B.C. Brown, H. Van-Leesten, R. Wickenberg's group, J.D. Wildenradt's group, J.R. Lackey, R.C. Webber, and F. Markley.

One of us, C. Hojvat would like to thank his Chinese colleagues for their will and dedication to make this project a reality. Their warmth, kindness and understanding have strengthened our mutual spirit of friendship, making ours a long lasting relationship. The whole of the Beijing accelerator project is a large and complex undertaking. One can only wish our colleagues many years of hard work and the successful utilization of their future accelerator for fundamental research.

We, the members of the Beijing Booster Injection Group, would like to express our deepest thanks to Dr. C. Hojvat and his colleagues D. Cosgrove and K. Bourkland for their valuable instruction and guidance in this work. Dr. C. Hojvat not only conducted the whole design but gave us assistance in all aspects of our stay at Fermilab.